

Syntheses and structural characterizations of novel mono- and dinuclear iridium hydrido complexes with polydentate nitrogen donor ligands

Masahiko Maekawa ^{a,*}, Toshie Minematsu ^b, Hisashi Konaka ^c, Kuniyoshi Sugimoto ^d, Takayoshi Kuroda-Sowa ^c, Yusaku Suenaga ^c, Megumu Munakata ^c

^a Research Institute for Science and Technology, Kinki University, 3-4-1 Kowakae, Higashi-Osaka, Osaka 577-8502, Japan

^b School of Pharmaceutical Sciences, Kinki University, Kowakae, Higashi-Osaka, Osaka 577-8502, Japan

^c Department of Chemistry, Kinki University, Kowakae, Higashi-Osaka, Osaka 577-8502, Japan

^d Rigaku Corporation, Matsubara-cho, Akishima, Tokyo 196-8666, Japan

Received 14 November 2003; accepted 24 March 2004

Available online 15 June 2004

Abstract

New five mono- and dinuclear Ir hydrido complexes with polydentate nitrogen ligands, $[\text{Ir}(\text{H})_2(\text{PPh}_3)_2(\text{tptz})]\text{PF}_6$ (**1**), $[\text{Ir}_2(\text{H})_4(\text{PPh}_3)_4(\text{tptz})](\text{PF}_6)_2 \cdot 2\text{H}_2\text{O}$ (**2** · $2\text{H}_2\text{O}$), $[\text{Ir}(\text{H})_2(\text{PPh}_3)_2(\text{tppz})]\text{BF}_4$ (**3**), $[\text{Ir}_2(\text{H})_4(\text{PPh}_3)_4(\text{tppz})](\text{BF}_4)_2$ (**4**) and $[\text{Ir}_2(\text{H})_4(\text{PPh}_3)_4(\text{bted})](\text{BF}_4)_2 \cdot 6\text{CHCl}_3$ (**5** · 6CHCl_3), were systematically prepared by the reactions of the precursor Ir hydrido complex $[\text{Ir}(\text{H})_2(\text{PPh}_3)_2(\text{Me}_2\text{CO})_2]\text{X}$ (X = PF_6 and BF_4) with 2,4,6-tris(2-pyridyl)-1,3,5-triazine (tptz), 2,3,5,6-tetrakis(2-pyridyl)pyrazine (tppz) and 1,4-bis(2,2':6',2''-terpyridine-4'-yl)benzene (bted), and their structures and properties were characterized in the solid state and in solution. Each of the Ir hydrido complexes with polydentate nitrogen ligands crystallographically described a unique coordination mode. Their ¹H NMR spectra demonstrated unusual ¹H NMR chemical shifts of pyridyl rings that are likely induced by the ring current effect of neighboring ligands.

© 2004 Elsevier B.V. All rights reserved.

Keywords: Iridium complexes; Hydrido complexes; Polydentate nitrogen ligands; Crystal structures; 2D NMR

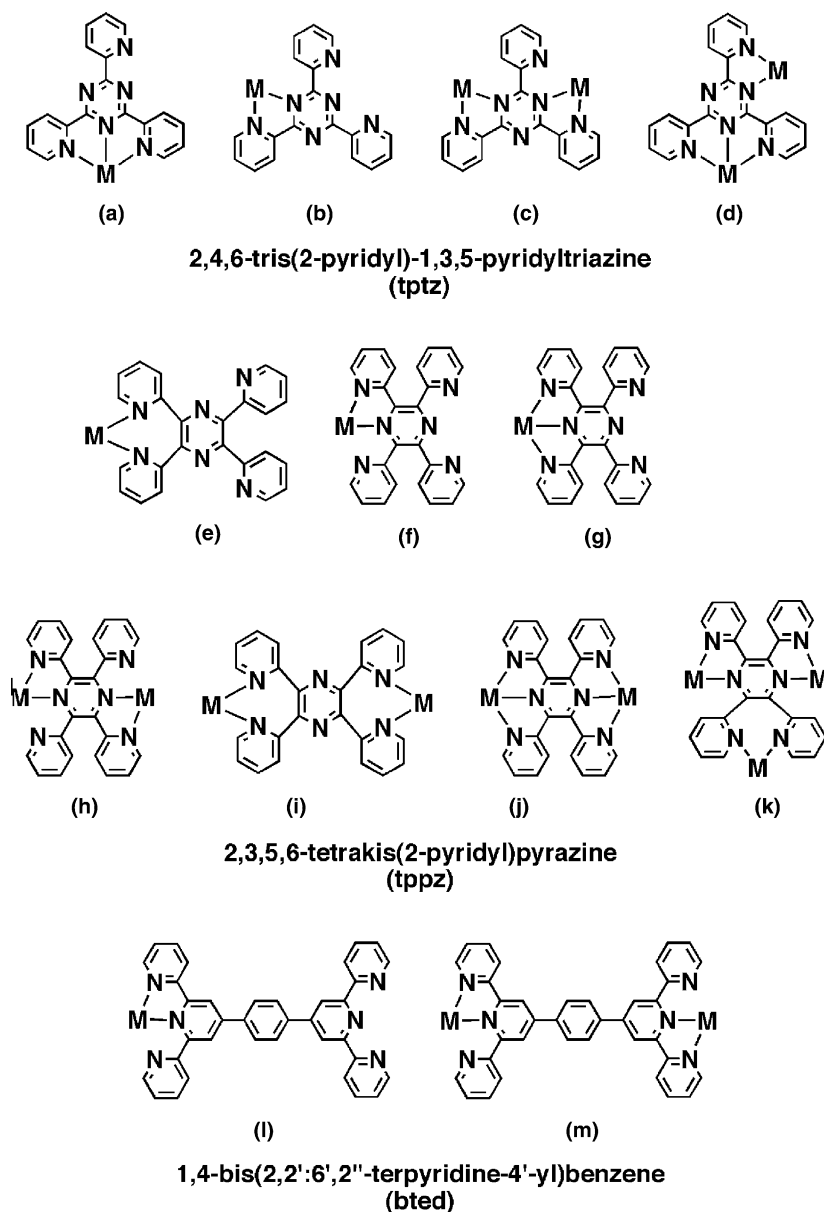
1. Introduction

In recent years, polynuclear metal complexes with aromatic nitrogen heterocycles as bridging ligands have been desirable for use in the study of photo-induced applications [1a–1d], extraction reagents [2a,2b] and specific catalytic reactions [3a–3e]. The design of these metal complexes requires N-donor bridging ligands having two or more bidentate sets of coordination sites to incorporate molecular components. For instance, the ligands 2,4,6-tris(2-pyridyl)-1,3,5-triazine (tptz), 2,3,5,6-tetrakis(2-pyridyl)pyrazine (tppz) and 1,4-bis(2,2':6',2''-terpyridine-4'-yl)benzene (bted) have been utilized as

polydentate nitrogen ligands to provide mono- and dinuclear metal complexes in various coordination modes (Scheme 1). In particular, the tptz ligand is the best potential polydentate pyridyl ligand since it has thus far been used as an analytical reagent for various metal ions [4a,4b]. The tptz ligand that can function simultaneously as bidentate and tridentate ligands has attracted considerable interest because of their potential use as spacers in the design of supramolecular complexes [5a–5d]. A number of transition metal and lanthanide complexes with the tptz ligand have been prepared. Mononuclear tptz complexes of Sm, Eu, Pr, Rh, Ru and Pb have been structurally characterized in the coordination mode (a) [3a,3c,6a–6d]. However, a mononuclear tptz complex in the coordination mode (b) has only been presented in a Re complex [3e]. A few dinuclear tptz complexes in the coordination modes (c) [3d,3e] and

* Corresponding author. Tel.: +81-6-6721-2332x4714; fax: +81-6-6730-5896.

E-mail address: maekawa@rist.kindai.ac.jp (M. Maekawa).



Scheme 1. The known coordination modes of metal complexes with polydentate nitrogen ligands.

(d) [5c] have been found in Ru, Os and Re complexes. More recently, it has been reported that interesting hydrolysis [3a,3b,3c], hydroxylation [3d] and methoxylation [3e] in tptz complexes of Rh, Ru and Os occurred on reflux in ethanol–water. On the other hand, the tppz ligand was synthesized by Goodwin et al. in the 1950s [7]. There have been reports on the synthesis and characterization of mononuclear tppz complexes of Re, Cu, Ru, Fe, Zn, Ir and Ni in the coordination modes (e) [8], (g) [9a–9f] and (f) [8,10]. Homobimetallic dinuclear tppz complexes of Pd, Cu, Ru, Ni, Zn and Co in the coordination mode (j) [9a,9d,11a–11h] have also been observed. However, observation of dinuclear tppz complexes in the coordination modes (h) [8] and (i) [12] and trinuclear tppz complex in the coordination mode

(k) [8] has been quite limited. Finally, the bted ligand has been of interest in the study of photo-induced applications due to its relationship to the tptz and tppz polydentate nitrogen ligands. However, our survey in SciFinder shows no crystallographic study of metal bted complexes. There have been a few structural NMR studies of the mononuclear Pt bted complex in the coordination mode (l) [13] and dinuclear bted complexes of Rh, Ir, Re and Ru in the coordination mode (m) [13,14a,14b]. Altogether, the preparative and structural studies of metal complexes with polydentate pyridyl ligands have not been sufficiently thorough.

We have recently been interested in exploring Rh and Ir complexes with bi- and polydentate nitrogen ligands to prepare mono- and dinuclear complexes with

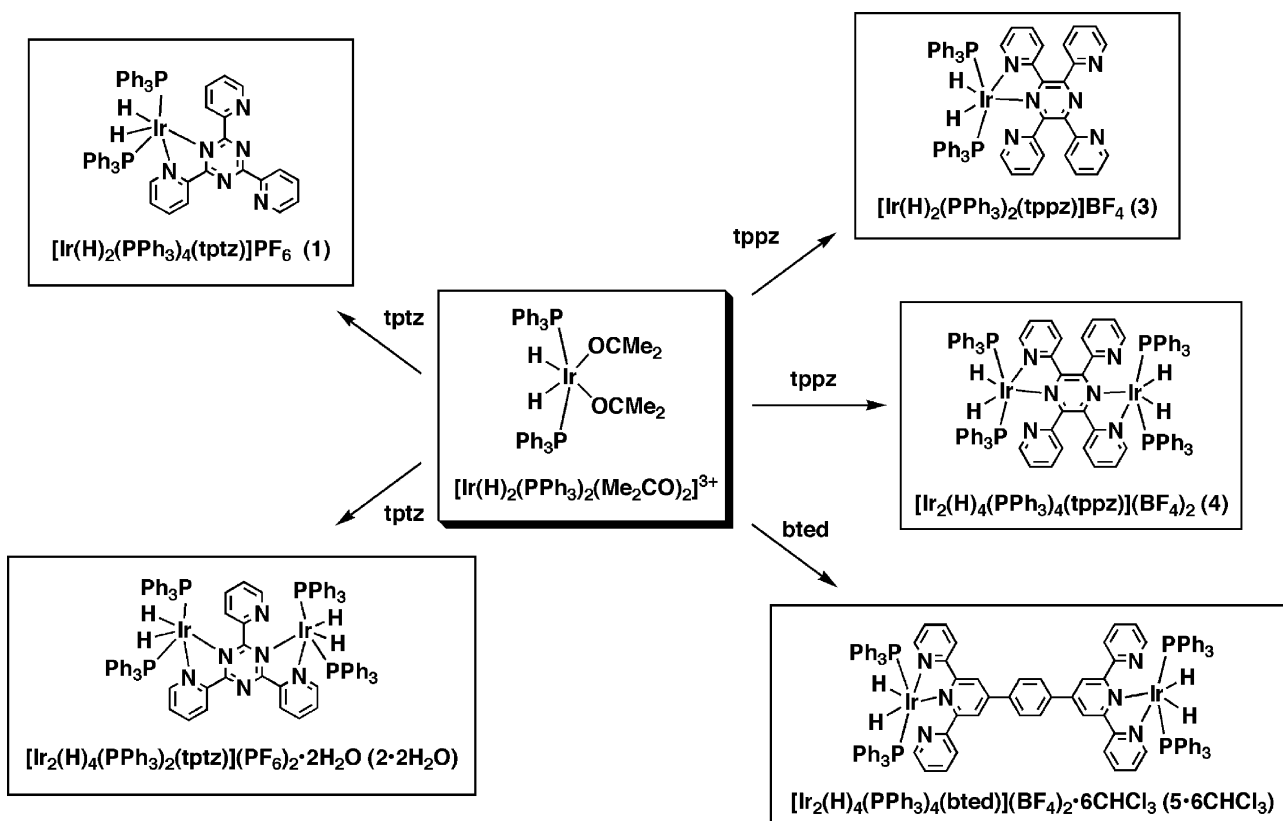
functions that can be utilized as building blocks to develop a supramolecular system. Because Rh and Ir hydrido complexes of formula $[M(H)_2(L)_2(solvent)_2]X$ ($M = Rh$ and Ir ; $L =$ phosphine ligand) have been found to be active catalysts [15] if the thus-reactive Rh or Ir metal centers can be joined by the N,N' -donor bridging ligands, these complexes are expected to produce coordination polymers with interesting structures and superior reactivities and properties due to a cooperative effect of the assembled metal site. We have examined the reactions of Rh and Ir hydrido complex $[M(H)_2(PPh_3)_2(EtOH)_2]X$ ($M = Rh$ and Ir ; $X = ClO_4$ and BF_4) with bidentate N,N' -donor bridging ligands such as pyrazine and 4,4'-bipyridine derivatives in various organic solvents [16a,16b,16c]. It has been illustrated that these reaction processes are closely related to the solvents and the structural feature of nitrogen-bridging ligands, resulting in the formation of unique dinuclear Rh and Ir complexes with hydrido or non-hydrido ligands. However, there still have been no investigative reports on the reaction of the Ir hydrido complex with a polydentate pyridyl ligand as described above. As such, the aim of the present study was to determine the reactions of the Ir hydrido complex $[Ir(H)_2(PPh_3)_2(Me_2CO)_2]X$ ($X = PF_6$ and BF_4) with tptz, tppz and bted ligands as polydentate nitrogen ligands, according to Scheme 2. A series of mono- and dinuclear Ir hydrido

complexes with polydentate nitrogen ligands $[Ir(H)_2(PPh_3)_2(tptz)]PF_6$ (**1**), $[Ir_2(H)_4(PPh_3)_4(tptz)](PF_6)_2 \cdot 2H_2O$ ($2 \cdot 2H_2O$), $[Ir(H)_2(PPh_3)_2(tppz)]BF_4$ (**3**), $[Ir_2(H)_4(PPh_3)_4(tppz)](BF_4)_2$ (**4**) and $[Ir_2(H)_4(PPh_3)_4(bted)](BF_4)_2 \cdot 6CHCl_3$ ($5 \cdot 6CHCl_3$) were obtained and their structures were crystallographically characterized. Their dynamic structures and spectroscopic properties were further examined by 1H NMR, UV-Vis and IR techniques in solution and in the solid state.

2. Experimental

2.1. General procedures and reagents

All procedures were carried out using standard Schlenk techniques under an argon atmosphere. $IrCl_3 \cdot 3H_2O$, 2,4,6-tris(2-pyridyl)-1,3,5-pyridyltriazine (tptz), 2,3,5,6-tetrakis(2-pyridyl)pyrazine (tppz) and 1,4-bis(2,2':6',2''-terpyridine-4'-yl)-benzene (bted) were purchased from Johnson–Matthey and Aldrich, and these chemicals were used without further purification. The precursor Ir hydrido complexes $[Ir(H)_2(PPh_3)_2(Me_2CO)_2]X$ ($X = PF_6$ and BF_4) were prepared according to the literature [17a,17b], with some modifications. All organic solvents were generally dried and distilled before use. IR spectra were measured on a JASCO FT/IR-430



Scheme 2.

spectrometer as a KBr pellet. UV–Vis spectra in the solid state were measured on a SHIMAZU UV-2450 spectrometer as a KBr pellet. The 1-D and 2-D NMR spectra were measured at room temperature and at $-90\text{ }^{\circ}\text{C}$ on JEOL ECA-500 and ECA-700 FT NMR spectrometers. Trimethylsilane was used as an internal reference for ^1H NMR measurements.

2.2. Syntheses

2.2.1. $[\text{Ir}(\text{H})_2(\text{PPh}_3)_2(\text{tptz})]\text{PF}_6$ (**1**)

A 5 ml THF solution of $[\text{Ir}(\text{H})_2(\text{PPh}_3)_2(\text{Me}_2\text{CO})_2]\text{PF}_6$ (49.0 mg, 0.05 mmol) was added to tptz (15.6 mg, 0.05 mmol) in THF (5 ml). After stirring for 15 min, the reaction solution was filtered. The light-yellow filtrates were placed in 5-mm diameter glass tubes and layered with pentane. The glass tubes were sealed and allowed to stand at room temperature for 3 days. Yellow brick crystals were collected. Yield. 32 mg (54%). *Anal.* Calc. for $\text{IrP}_3\text{F}_6\text{C}_{54}\text{H}_{44}\text{N}_6$: C, 55.15; H, 3.77; N, 7.15. Found: C, 54.87; H, 3.88; N, 7.01%. IR(KBr pellet, cm^{-1}): 2250 (Ir–H), 2205 (Ir–H), 1572, 1544, 1505, 1481, 1435, 1402, 1384, 1358 and 840 (PF_6^-). UV–Vis(KBr pellet, nm): 400 and 480.

2.2.2. $[\text{Ir}_2(\text{H})_4(\text{PPh}_3)_4(\text{tptz})](\text{PF}_6)_2 \cdot 2\text{H}_2\text{O}$ (**2**· $2\text{H}_2\text{O}$)

Complex **2**· $2\text{H}_2\text{O}$ was prepared by the reaction of $[\text{Ir}(\text{H})_2(\text{PPh}_3)_2(\text{Me}_2\text{CO})_2]\text{PF}_6$ (98.0 mg, 0.10 mmol) with tptz (15.6 mg, 0.05 mmol) in THF (10 ml) in the same manner as for **1**. Red brick crystals of **2**· $2\text{H}_2\text{O}$ were obtained at room temperature after 3 days. Yield. 50 mg (48%). *Anal.* Calc. for $\text{Ir}_2\text{P}_6\text{F}_{12}\text{O}_2\text{N}_6\text{C}_{90}\text{H}_{80}$: C, 52.99; H, 3.76; N, 4.12. Found: C, 53.01; H, 4.13; N, 3.91%. IR(KBr, cm^{-1}): 2248 (Ir–H), 1529, 1482, 1435 and 840 (PF_6^-). UV–Vis(KBr pellet, nm): 430 and 510.

2.2.3. $[\text{Ir}(\text{H})_2(\text{PPh}_3)_2(\text{tppz})]\text{BF}_4$ (**3**)

A 5 ml Me_2CO solution of $[\text{Ir}(\text{H})_2(\text{PPh}_3)_2(\text{Me}_2\text{CO})_2]\text{BF}_4$ (46.1 mg, 0.05 mmol) was added to tppz (9.7 mg, 0.05 mmol) in Me_2CO (5 ml). After stirring for 15 min, the reaction solution was filtered. The orange filtrates were placed in 5-mm diameter glass tubes and layered with pentane. The glass tubes were sealed and the solution was allowed to stand at room temperature for 3 days. Orange plate crystals of **3** were obtained. Yield. 33 mg (56%). *Anal.* Calc. for $\text{IrP}_2\text{F}_4\text{N}_6\text{C}_{60}\text{BH}_{48}$: C, 60.35; H, 4.05; N, 7.04. Found: C, 58.45; H, 3.93; N, 7.48%. IR(KBr pellet, cm^{-1}): 2291 (Ir–H), 2192 (Ir–H), 1586, 1568, 1480, 1434, 1393 and 1058 (BF_4^-). UV–Vis(KBr pellet, nm): 360 and 465.

2.2.4. $[\text{Ir}_2(\text{H})_4(\text{PPh}_3)_4(\text{tppz})](\text{BF}_4)_2$ (**4**)

In the same manner as for **3**, complex **4** was synthesized by the reaction of $[\text{Ir}(\text{H})_2(\text{PPh}_3)_2(\text{Me}_2\text{CO})_2]\text{BF}_4$

(92.2 mg, 0.10 mmol) with tppz (9.7 mg, 0.05 mmol) in CH_2Cl_2 (10 ml). Dark-red brick crystals were collected at room temperature 3 days later. Yield. 45 mg (45%). *Anal.* Calc. for $\text{Ir}_2\text{P}_4\text{F}_8\text{N}_6\text{C}_{96}\text{B}_2\text{H}_{80}$: C, 57.66; H, 4.03; N, 4.20. Found: C, 56.93; H, 4.13; N, 4.21%. IR(KBr pellet, cm^{-1}): 2284 (Ir–H), 2233 (Ir–H), 1586, 1480, 1434, 1385 and 1057 (BF_4^-). UV–Vis(KBr pellet, nm): 375 and 535.

2.2.5. $[\text{Ir}_2(\text{H})_4(\text{PPh}_3)_4(\text{bted})](\text{BF}_4)_2 \cdot 6\text{CHCl}_3$ (**5**· 6CHCl_3)

$[\text{Ir}(\text{H})_2(\text{PPh}_3)_2(\text{Me}_2\text{CO})_2]\text{BF}_4$ (46.1 mg, 0.05 mmol) and bted (27.0 mg, 0.05 mmol) were mixed in CHCl_3 (10 ml) overnight and the suspension solution was filtered. The pale-yellow filtrates were placed in 5-mm diameter glass tubes and layered with hexane. The glass tubes were sealed and the solution was allowed to stand at room temperature for 3 days. Yellow brick crystals of **5**· 6CHCl_3 were collected. Yield. 40 mg (28%). *Anal.* Calc. for $\text{Ir}_2\text{Cl}_{18}\text{P}_4\text{F}_8\text{N}_6\text{C}_{114}\text{B}_2\text{H}_{94}$: C, 57.66; H, 4.03; N, 4.20. Found: C, 56.93; H, 4.13; N, 4.21%. IR(KBr pellet, cm^{-1}): 2282 (Ir–H), 1617, 1481, 1434 and 1083 (BF_4^-). UV–Vis(KBr pellet, nm): 310 and 400.

The detailed NMR data of complexes **1**–**5**· 6CHCl_3 are summarized in Table 4 together with other spectroscopic data.

2.3. X-ray data collection and structure solution

For each Ir hydrido complex of **1**–**5**· 6CHCl_3 , a suitable crystal was mounted on a glass fiber. The X-ray measurements for **1**, **2**· $2\text{H}_2\text{O}$ and **3** were made on a Rigaku/MSC Mercury CCD diffractometer with graphite-monochromated Mo $\text{K}\alpha$ radiation ($\lambda = 0.71069\text{ \AA}$) at $-123\text{ }^{\circ}\text{C}$ for **1** and **3** and at $-150\text{ }^{\circ}\text{C}$ for **2**· $2\text{H}_2\text{O}$. The measurements for **4** and **5**· 6CHCl_3 were made on a Quantum CCD detector coupled with a Rigaku AFC-8 diffractometer with graphite-monochromated Mo $\text{K}\alpha$ radiation ($\lambda = 0.71069\text{ \AA}$) at $-123\text{ }^{\circ}\text{C}$. The structures of **1**, **2**· $2\text{H}_2\text{O}$, **3**, **4** and **5**· 6CHCl_3 were solved by a direct method (*SAPI-91* for **1**, **4** and **5**· 6CHCl_3 ; *SIR-92* for **3**) [18]. All of the structures were expanded using Fourier techniques [19]. The two hydrido atoms were located at the calculated positions in **1** and **2**· $2\text{H}_2\text{O}$, whereas they were located from a density map and refined isotropically in **3**, **4** and **5**· 6CHCl_3 . In complex **2**· $2\text{H}_2\text{O}$, one phenyl group including C(1)–C(6) atoms and one pyridyl group including N(4) and C(44)–C(48) atoms were treated as ideal models and were isotropically refined. The C(43) atom of triazine ring and the O(1) atom of H_2O molecule were isotropically refined. In all complexes **1**–**5**· 6CHCl_3 all other hydrogen atoms were placed at the calculated positions and were included, but not refined. The atomic-scattering factors and anomalous dispersion terms were taken

Table 1
Crystallographic data for mono- and dinuclear Ir hydrido complexes with polydentate nitrogen ligands, 1–5 · 6CHCl₃

	[Ir(H) ₂ (PPh ₃) ₂ - (tptz)]PF ₆ (1)	[Ir ₂ (H) ₄ (PPh ₃) ₄ (tptz)]- (PF ₆) ₂ · 2H ₂ O (2 · 2H ₂ O)	[Ir(H) ₂ (PPh ₃) ₂ - (tppz)]BF ₄ (3)	[Ir ₂ (H) ₄ (PPh ₃) ₄ - (tppz)](BF ₄) ₂ (4)	[Ir ₂ (H) ₄ (PPh ₃) ₄ (bted)]- (BF ₄) ₂ · 6CHCl ₃ (5 · 6CHCl ₃)
Formula	IrP ₃ F ₆ C ₅₄ H ₄₄ N ₆	Ir ₂ P ₆ F ₁₂ O ₂ N ₆ C ₉₀ H ₈₀	IrP ₂ F ₄ N ₆ C ₆₀ BH ₄₈	Ir ₂ P ₄ F ₈ N ₆ C ₉₆ B ₂ H ₈₀	Ir ₂ Cl ₁₈ P ₄ F ₈ N ₆ C ₁₁₄ B ₂ H ₉₄
Formula weight	1176.11	2075.92	1194.05	1999.67	2868.13
Crystal system	orthorhombic	monoclinic	triclinic	triclinic	triclinic
Space group	<i>P</i> 2 ₁ 2 ₁ 2 ₁	<i>C</i> 2	<i>P</i> $\bar{1}$	<i>P</i> $\bar{1}$	<i>P</i> $\bar{1}$
<i>a</i> (Å)	16.842(4)	24.420(8)	13.946(6)	12.2187(9)	11.7996(5)
<i>b</i> (Å)	16.624(4)	15.445(4)	14.136(6)	13.106(1)	15.666(2)
<i>c</i> (Å)	17.544(4)	18.629(6)	15.410(6)	14.025(1)	16.587(1)
α (°)			106.646(4)	91.802(1)	93.435(2)
β (°)		137.769(4)	90.151(1)	97.071(1)	102.2082(5)
γ (°)			115.860(5)	112.987(2)	94.7508(8)
<i>V</i> (Å ³)	4912(2)	4722(2)	2590(1)	2044.2(3)	2977.2(4)
<i>Z</i>	4	2	2	1	1
μ (Mo K α) (cm ⁻¹)	28.91	29.96	2.707	34.11	27.58
Temperature (K)	150	123	150	150	150
No. of reflections measured	38 778 (total); 6134 (unique)	18 720 (total); 5589 (unique)	30 359 (total); 11 742 (unique)	23 984 (total); 9276 (unique)	49 234 (total); 13 681 (unique)
No. of reflections	10 291 (all data)	10 630 (all data)	10 296 (all data)	8772 (all data)	12 811 (all data)
<i>R</i>	0.034 ^a	0.078, ^b 0.047(<i>I</i> > 2.0 σ (<i>I</i>)) ^c	0.037 ^a	0.020 ^a	0.035 ^a
<i>R</i> _w	0.059 ^d	0.118 ^d	0.071 ^d	0.047 ^d	0.090 ^d

$$^a R = \sum ||F_o| - |F_c|| / \sum |F_o|.$$

$$^b R = \sum (F_o^2 - F_c^2) / \sum F_o^2.$$

$$^c R1 = \sum ||F_o| - |F_c|| / \sum |F_o|.$$

$$^d R_w = [\sum w(F_o^2 - F_c^2)^2 / \sum w(F_o^2)]^{1/2}.$$

from [20]. All of the calculations were performed using the TEXSAN crystallographic software package of Molecular Structure Corporation [21]. Crystal data and details of the structure determination are summarized in Table 1.

3. Results and discussion

3.1. Preparations and spectroscopic data

As mentioned in Section 1, the tptz ligand generally can provide tptz complexes with several coordination modes (a)–(d) in Scheme 1. However, there are still no reports of an Ir complex with the tptz ligand. Attempts at carrying out stoichiometric 1:1 and 2:1 reactions of the precursor Ir hydrido complex [Ir(H)₂(PPh₃)₂-(Me₂CO)₂]PF₆ and tptz in THF afforded yellow and red crystals that were later crystallographically characterized as mononuclear complex [Ir(H)₂(PPh₃)₂(tptz)]PF₆ (**1**) and dinuclear complex [Ir₂(H)₄(PPh₃)₄(tptz)]-(PF₆)₂ · 2H₂O (**2** · 2H₂O), respectively. Excess addition of the precursor Ir hydrido complex only provided red brick crystals of **2** · 2H₂O, suggesting that the dinuclear structure in the coordination mode (c) is preferable to the other coordination modes and that a trinuclear structure could not be formed due to the steric effects between tptz and PPh₃ ligands. A similar suggestion has been made regarding the formation process of the di-

nuclear Re tptz complex [3e]. The UV–Vis spectra of **1** and **2** · 2H₂O in the solid state are provided in Fig. 1. Mononuclear complex **1** gave two absorptions at 400 and 480 nm, whereas dinuclear complex **2** · 2H₂O exhibited two absorptions at 430 and 510 nm. It is interesting that the UV–Vis spectra of mononuclear and dinuclear complexes show significant differences: the absorption of dinuclear complex **2** · 2H₂O exhibits a significant red-shift (30 nm) compared to that of mononuclear complex **1**. These absorptions were assigned as the d π (Ir) \rightarrow π^* (tptz) charge-transfer transition (MLCT) on the basis of the assignments of mono- and dinuclear tptz complexes of Ru, Os and Re [3d,3e]. Generally, it has been reported that the addition of a second metal ion at the remote coordination site of the bridging ligand results in stabilization of the π^* level of the bridging ligand, leading to d π \rightarrow π^* orbital overlap. This effect lowers the HOMO–LUMO gap, resulting in a low-energy shift of the MLCT bands in the dinuclear complexes. Our observation in this study is quite consistent with other reports of tptz complexes of Ru, Os and Re [3d,3e].

Similarly, the stoichiometric 1:1 and 2:1 reactions of the precursor Ir hydrido complex [Ir(H)₂(PPh₃)₂-(Me₂CO)₂]BF₄ and tppz ligand provided orange crystals of mononuclear complex [Ir(H)₂(PPh₃)₂(tppz)]BF₄ (**3**) and dark-red crystals of dinuclear complex [Ir₂(H)₄(PPh₃)₄(tppz)](BF₄)₂ (**4**), respectively. Excess addition of the precursor Ir hydrido complex only produced dinuclear complex **4** as well as complex **2** · 2H₂O.

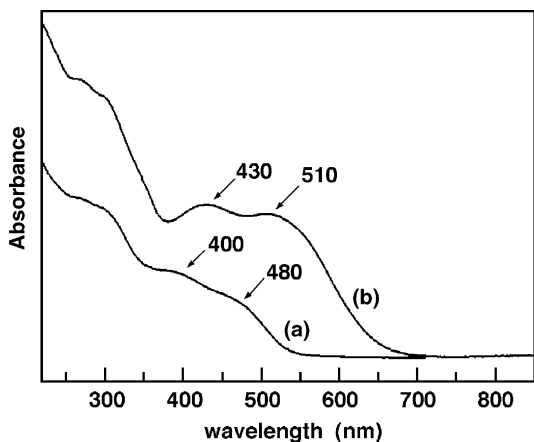


Fig. 1. UV-Vis spectra of $[\text{Ir}(\text{H})_2(\text{PPh}_3)_2(\text{tptz})]\text{PF}_6$ (**1**) (a) and $[\text{Ir}_2(\text{H})_4(\text{PPh}_3)_4(\text{tptz})](\text{PF}_6)_2 \cdot 2\text{H}_2\text{O}$ (**2**· $2\text{H}_2\text{O}$) (b) as a KBr pellet in the solid state.

This result suggests that the dinuclear structure in the coordination mode (h) should be selectively produced among several coordination modes (h)–(k) due to the steric effects between tppz and PPh_3 ligands without formation of another polynuclear species. Complexes **3** and **4** in the solid state exhibited broad absorptions at {360 and 465} and {375 and 535} nm, respectively, which are assigned as the MLCT band according to other tppz complexes [9e,11c,11g]. Similar to the above Ir tptz complexes **1** and **2**, the meaningful red-shifts ($\Delta\delta = 15$ and 70 nm) could be confirmed in Ir tppz complexes **3** and **4**, accompanying by formation of a dinuclear complex.

Finally, the bted ligand is relatively insoluble in general organic solvents. We could not perform the stoichiometric reaction of the precursor Ir hydrido complex $[\text{Ir}(\text{H})_2(\text{PPh}_3)_2(\text{Me}_2\text{CO})_2]\text{BF}_4$ and the bted ligand. However, the precursor Ir hydrido complex and bted were stirred in CHCl_3 overnight and the yellow suspension was then filtrated. Yellow brick crystals of dinuclear complex **5**· 6CHCl_3 were collected from the diffusion solution of the filtrates. It is therefore thought that dinuclear complex **5**· 6CHCl_3 was deposited as the most low-soluble and stable species in the reaction solution. Although a small number of apparently red crystals were sometimes collected in the same sample tubes, the red crystals were crystallographically identical to the yellow crystals of **5**· 6CHCl_3 . At the present time, we have not isolated the formation of any other species. Dinuclear complex **5**· 6CHCl_3 exhibited two absorptions at 310 and 400 nm in the solid state.

Complex **1** showed well-resolved Ir–H stretching vibrations at {2250 and 2205} cm^{-1} . Complexes **2**· $2\text{H}_2\text{O}$, **3**, **4** and **5**· 6CHCl_3 also gave the Ir–H stretching vibrations at 2248, {2291 and 2192}, {2284 and 2233} and 2282 cm^{-1} , respectively. Generally, it has been known that metal complexes with hydrido and molecular hy-

drogen as a ligand should exhibit the characteristic infrared spectrum in the range of 1500–2300 ($\nu(\text{M}-\text{H})$) and {2400 – 3100 ($\nu(\text{H}-\text{H})$) and 850–950 ($\nu_s(\text{M}-(\text{H}_2))$)} cm^{-1} [22a,22b], depending on the coordination modes of H–M–H and M–(H_2), respectively. When it is difficult to crystallographically determine the coordination mode of the coordinating hydrogen atom, the IR measurement is utilized as the most convenient analytical method to characterize a hydrido complex in the solid state, in addition to NMR techniques in solution. As shown in Section 2, all of the Ir–H stretching absorptions in complexes **1**–**5**· 6CHCl_3 were within the range found in Ir hydrido complexes with the M–H mode. These IR data support each of the structures established in the following X-ray crystal structure determinations. These spectroscopic data are summarized in Table 4 together with the ^1H NMR data.

3.2. Crystal structures

3.2.1. $[\text{Ir}(\text{H})_2(\text{PPh}_3)_2(\text{tptz})]\text{PF}_6$ (**1**)

The 1:1 reaction of $[\text{Ir}(\text{H})_2(\text{PPh}_3)_2(\text{Me}_2\text{CO})_2]\text{PF}_6$ and tptz in THF afforded yellow crystals of **1**. The crystal structure of **1** is shown in Fig. 2 together with the atomic labeling scheme. The Ir atom is coordinated by the two N atoms among the six potentially coordinative N atoms of tptz to provide a mononuclear structure in the coordination mode (b). The Ir atom is also coordinated by two *trans* PPh_3 ligands and two *cis* hydrido ligands in a distorted octahedral geometry. The two *cis* hydrido atoms are located at the calculated positions, which were confirmed by the IR determinations described above. To our knowledge, the tptz ligand can produce various tptz complexes in

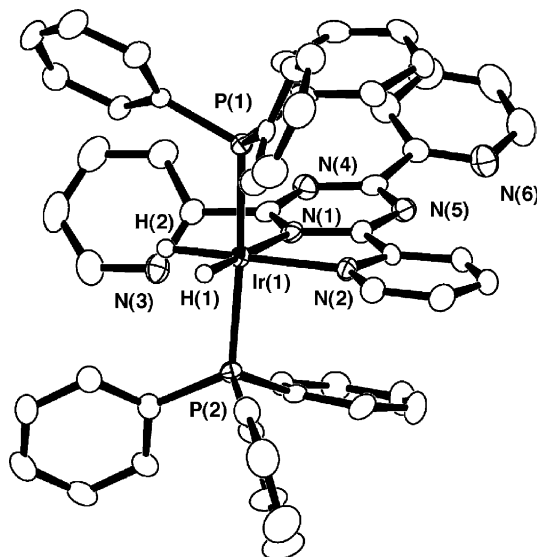


Fig. 2. The X-ray crystal structure of $[\text{Ir}(\text{H})_2(\text{PPh}_3)_2(\text{tptz})]\text{PF}_6$ (**1**).

coordination modes (a)–(d). Our survey in SciFinder indicates that most mononuclear tptz complexes have been structurally characterized in the coordination mode (a): [Ru(tptz)₂][PF₆ · H₂O] [3a], [Rh(tptz)Cl₃]₂ · 2H₂O [3c], [Sm(NO₃)₃(tptz)(H₂O)] · 2H₂O [6a], [Eu(tptz)Cl₃(MeOH)₂] · MeOH [6b], [Pr(tptz)Cl₃(OAc)₃]₂ · 2MeOH [6b], [Pb(tptz)X₂] · solvent (X = Cl, Br, I and SCN) [6c], [Pb(tptz)(NO₃)₂] · solvent [6c] and [Ni(tptz)(H₂O)₃](NO₃)₃ · H₂O [6d]. In contrast, the Re complex [ReX(CO)₃-(tptz)] (X = Cl and Br) [3e] has only been presented as a mononuclear tptz complex in the coordination mode (b), in addition to a few examples of dinuclear complexes [M(bpy)₂]₂(tptz-OH)(PF₆)₃ · H₂O (M = Ru and Os) [3d] and (μ-tptz)[ReX(CO)₃]₂ (X = Cl and Br) [3e] in the coordination mode (c) and [Ru(tpy)(tptz)](ClO₄)₂ · 0.5AgClO₄ · 2H₂O [5c] in the coordination mode (d). Therefore, complex **1** is the first mononuclear Ir tptz complex to be presented in the coordination mode (b). This structural feature is greatly different from the coordination mode (a) of the Rh tptz complex [Rh(tptz)Cl₃]₂ · 2H₂O [3c], which has only been reported as an homologous complex.

The average Ir–P and Ir–N distances of 2.311 and 2.166 Å are within those of other Ir hydrido complexes with a nitrogen donor ligand [16b]. The P(1)–Ir(1)–P(2) and N(1)–Ir(1)–N(2) angles are 173.22(4)° and 76.8(1)°, respectively. In the metal-free tptz ligand, it has been reported that the dihedral angles between the three pyridyl groups and the central triazine ring are 15.7(1)°, 19.8(1)° and 33.8(1)°, respectively [23]. In the similar Re complexes [ReX(CO)₃(tptz)] (X = Cl and Br) [3e], the dihedral angles between the coordinated pyridyl ring (A) and the central triazine ring (D) are 9.0 (X = Cl) and 8.4° (X = Br), respectively. The dihedral angles between the uncoordinated pyridyl ring (B) and the central triazine ring (D) are 45.3 (X = Cl) and 43.2° (X = Br), respectively. In contrast, in our complex **1**, the dihedral angle between the coordinated pyridyl ring (A) and the central triazine ring (D) is 6.83°, which is slightly smaller than those (9.0° and 8.4°) of the above [ReX(CO)₃(tptz)] complex [3e]. The uncoordinated pyridyl ring (B) is considerably twisted 45.67° from the central triazine ring (D) to minimize the steric interaction from the adjacent Ir fragment, compared with the interaction (19.86°) between the coordinated pyridyl ring (C) and the central triazine ring (D). The selected bond distances, bond angles and dihedral angles of **1** are listed in Tables 2 and 3, respectively.

3.2.2. [Ir₂(H)₄(PPh₃)₄(tptz)](PF₆)₂ · 2H₂O (2 · 2H₂O)

The 2:1 reaction of [Ir(H)₂(PPh₃)₂(Me₂CO)₂][PF₆] and tptz in THF afforded red brick crystals of **2** · 2H₂O. The crystal structure of **2** · 2H₂O is shown in Fig. 3 together with the atomic labeling scheme. There is one [Ir₂(H)₄(PPh₃)₄(tptz)](PF₆)₂ complex and two solvated

H₂O molecules in the unit cell. The solvated H₂O molecules exhibited no specific interaction such as a hydrogen bond. The two Ir atoms are bridged by the four N atoms among the six possibly coordinative N atoms of tptz to provide a dinuclear structure in the coordination mode (c). Here, in contrast to complex **1**, the tptz ligand acts as a bridging ligand. Each of the Ir atoms is coordinated by two *trans* PPh₃ ligands and two *cis* hydrido ligands in a distorted octahedral geometry. The two *cis* hydrido atoms are located at the calculated positions. Regarding a dinuclear complex of tptz, it has been known that there are a few tptz complexes of Ru and Re, [M(bpy)₂]₂(tptz-OH)(PF₆)₃ · H₂O (M = Ru and Os) [3d] and (μ-tptz)[ReX(CO)₃]₂ (X = Cl and Br) [3e] in the coordination mode (c) and [Ru(tpy)(tptz)](ClO₄)₂ · 0.5AgClO₄ · 2H₂O [5c] in the coordination mode (d). Therefore, complex **2** · 2H₂O is the first identified dinuclear Ir tptz complex in the coordination mode (c).

The average Ir–P and Ir–N distances of 2.312 and 2.180 Å are similar to those of complex **1** and other Ir hydrido complexes with a nitrogen donor ligand [16b]. The P(1)–Ir(1)–P(2) of 164.7(1)° is smaller than the corresponding angle (173.22(4)°) of **1**, whereas the P(1)–Ir(1)–N(2) of 101.7(2)° is larger than that (91.17(8)°) of **1**, resulting in a decrease in repulsion with respect to PPh₃ groups on the neighboring Ir atom and pyridyl groups of the tptz ligand. The dihedral angle of 5.02° between the coordinated pyridyl rings {(A) and (B)} and the central triazine ring (D) is smaller than that (6.83°) of **1** and those (10.9° and 11.3°) of the similar Re complex [Re₂(Cl)₂(CO)₆(tptz)] [3e]. The [Ir₂(tptz)] coordination plane formed by two Ir atoms, two coordinated pyridyl groups {(A) and (B)} and the central triazine ring (D) is almost planar. In contrast, the dihedral angle of 79.45° between the uncoordinated pyridyl ring (C) and the central triazine ring (D) is larger than that (64.7°) of [Re₂(Cl)₂(CO)₆(tptz)] [3e]. It is interesting that the uncoordinated pyridyl ring (C) is almost located vertically against the [Ir₂(tptz)] coordination plane to minimize the steric interaction with respect to pyridyl and PPh₃ groups. The selected bond distances, bond angles and dihedral angles are listed in Tables 2 and 3, respectively.

3.2.3. [Ir(H)₂(PPh₃)₂(tppz)]BF₄ (**3**)

Similar to complex **1**, the 1:1 reaction of [Ir(H)₂(PPh₃)₂(Me₂CO)₂][BF₄] and tppz in Me₂CO provided orange crystals of **3**. The crystal structure of **3** is shown in Fig. 4 together with the atomic labeling scheme. The Ir atom is coordinated by the two N atoms among the six potentially coordinative N atoms of tppz to provide a mononuclear structure in the coordination mode (f). The Ir atom is bonded to two *trans* PPh₃ ligands and two *cis* hydrido ligands in a distorted octahedral

Table 2

Selected bond distances (Å) and bond angles (°) of mono- and dinuclear Ir hydrido complexes with polydentate nitrogen ligands, **1–5** · 6CHCl₃

<i>(a) [Ir(H)₂(PPh₃)₂(tptz)]PF₆ (1)</i>			
Ir(1)–P(1)	2.3092(9)	Ir(1)–P(2)	2.313(1)
Ir(1)–N(1)	2.171(3)	Ir(1)–N(2)	2.161(3)
Ir(1)–H(1) ^a	1.50	Ir(1)–H(2) ^a	1.50
P(1)–Ir(1)–P(2)	173.22(4)	P(1)–Ir(1)–N(1)	93.25(9)
P(1)–Ir(1)–N(2)	91.17(8)	P(2)–Ir(1)–N(1)	93.51(9)
P(2)–Ir(1)–N(2)	90.91(8)	N(1)–Ir(1)–N(2)	76.8(1)
<i>(b) [Ir₂(H)₄(PPh₃)₄(tptz)](PF₆)₂ · 2H₂O (2 · 2H₂O)</i>			
Ir(1)–P(1)	2.312(2)	Ir(1)–P(2)	2.311(2)
Ir(1)–N(1)	2.162(6)	Ir(1)–N(2)	2.20(1)
Ir(1)–H(39) ^a	1.50	Ir(1)–H(40) ^a	1.50
P(1)–Ir(1)–P(2)	164.7(1)	P(1)–Ir(1)–N(1)	93.7(2)
P(1)–Ir(1)–N(2)	101.7(2)	P(2)–Ir(1)–N(1)	91.7(2)
P(2)–Ir(1)–N(2)	93.5(2)	N(1)–Ir(1)–N(2)	75.8(3)
<i>(c) [Ir(H)₂(PPh₃)₂(tppz)]BF₄ (3)</i>			
Ir(1)–P(1)	2.317(1)	Ir(1)–P(2)	2.302(1)
Ir(1)–N(1)	2.155(4)	Ir(1)–N(3)	2.155(2)
Ir(1)–H(1)	1.45(4)	Ir(1)–H(2)	1.50(4)
P(1)–Ir(1)–P(2)	165.59(3)	P(1)–Ir(1)–N(1)	93.95(8)
P(2)–Ir(1)–N(3)	92.08(8)	P(2)–Ir(1)–N(1)	97.21(8)
P(2)–Ir(1)–N(3)	99.36(8)	N(1)–Ir(1)–N(3)	76.5(1)
P(1)–Ir(1)–H(1)	85(1)	P(1)–Ir(1)–H(2)	87(1)
P(2)–Ir(1)–H(1)	83(1)	P(2)–Ir(1)–H(2)	81(1)
N(1)–Ir(1)–H(1)	100(1)	N(1)–Ir(1)–H(2)	176(1)
N(3)–Ir(1)–H(1)	176(1)	N(3)–Ir(1)–H(2)	99(1)
H(1)–Ir(1)–H(2)	83(2)		
<i>(d) [Ir₂(H)₄(PPh₃)₄(tppz)](BF₄)₂ (4)</i>			
Ir(1)–P(1)	2.3184(7)	Ir(1)–P(2)	2.3113(7)
Ir(1)–N(1)	2.137(2)	Ir(1)–N(2)	2.220(2)
Ir(1)–H(1)	1.40(3)	Ir(1)–H(2)	1.37(3)
P(1)–Ir(1)–P(2)	160.20(2)	P(1)–Ir(1)–N(1)	97.48(6)
P(1)–Ir(1)–N(2)	103.24(6)	P(1)–Ir(1)–H(1)	80.7(11)
P(1)–Ir(1)–H(2)	75.0(11)	P(2)–Ir(1)–N(1)	91.70(6)
P(2)–Ir(1)–N(2)	96.03(6)	P(2)–Ir(1)–H(1)	91.3(11)
P(2)–Ir(1)–H(2)	86.0(11)	N(1)–Ir(1)–N(2)	75.32(6)
N(1)–Ir(1)–H(1)	175.6(10)	N(1)–Ir(1)–H(2)	101.3(11)
N(2)–Ir(1)–H(1)	101.1(11)	N(2)–Ir(1)–H(2)	176.0(11)
H(1)–Ir(1)–H(2)	82.2(15)		
<i>(e) [Ir₂(H)₄(PPh₃)₄(bted)](BF₄)₂ · 6CHCl₃ (5 · 6CHCl₃)</i>			
Ir(1)–P(1)	2.3027(8)	Ir(1)–P(2)	2.2969(9)
Ir(1)–N(1)	2.147(3)	Ir(1)–N(2)	2.168(3)
Ir(1)–H(1)	1.48(5)	Ir(1)–H(2)	1.34(5)
P(1)–Ir(1)–P(2)	161.84(3)	P(1)–Ir(1)–N(1)	98.43(8)
P(1)–Ir(1)–N(2)	94.88(8)	P(1)–Ir(1)–H(1)	83(1)
P(1)–Ir(1)–H(2)	83(2)	P(2)–Ir(1)–N(1)	94.33(8)
P(2)–Ir(1)–N(2)	100.54(8)	P(2)–Ir(1)–H(1)	81(1)
P(2)–Ir(1)–H(2)	86(2)	N(1)–Ir(1)–N(2)	77.1(1)
N(1)–Ir(1)–H(1)	98(1)	N(1)–Ir(1)–H(2)	175(2)
N(2)–Ir(1)–H(1)	175(1)	N(2)–Ir(1)–H(2)	98(2)
H(1)–Ir(1)–H(2)	86(3)		

^a The Ir–H distance is fixed as 1.50 Å.

geometry. To the best of our knowledge, several mononuclear tppz complexes have been structurally characterized as follows: [ReCl(CO)₃(tppz)] · 2H₂O [8] in

the coordination mode (e); [Cu₂Cl₂(tppz)] [9a], [Ru(tppz)(4,4'-Me₂bpy)Cl]PF₆ [9b], [Fe(tppz)₂][(di-pic)₂Fe]₃ · H₃O · 11H₂O [9c], [Zn(tppz)Cl]₂ [9d],

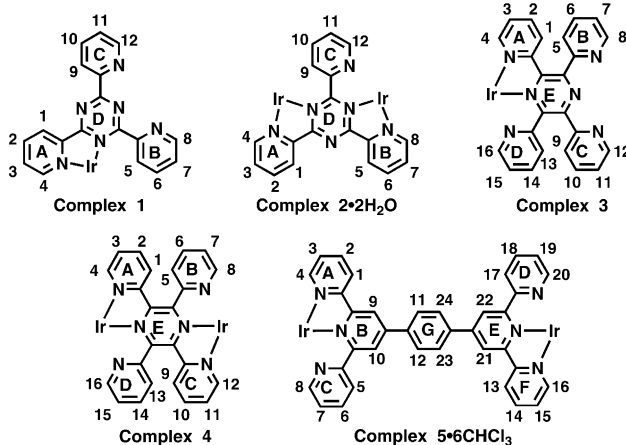
Table 3
Dihedral angles (°) of mono- and dinuclear Ir hydrido complexes with polydentate nitrogen ligands, 1–5 · 6CHCl₃

Complexes	Plane 1	Plane 2	Dihedral angles (°)	Plane 1	Plane 2	Dihedral angles (°)
[Ir(H) ₂ (PPh ₃) ₂ (tptz)]PF ₆ (1)	A	B	50.60	A	C	21.74
	A	D	6.83	B	D	45.67
	C	B	31.60	C	D	19.86
[Ir ₂ (H) ₄ (PPh ₃) ₄ (tptz)](PF ₆) ₂ · 2H ₂ O (2 · 2H ₂ O)	A	B	8.44	A	C	82.22
	A	D	5.02	B	D	5.02
	C	B	82.16	C	D	79.45
[Ir(H) ₂ (PPh ₃) ₂ (tppz)]BF ₄ (3)	A	B	69.15	A	E	12.06
	A	C	57.07	A	D	73.23
	B	C	78.00	B	D	51.93
	B	E	68.22	D	C	51.48
	E	C	45.08	E	D	67.58
[Ir ₂ (H) ₄ (PPh ₃) ₄ (tppz)](BF ₄) ₂ (4)	A	B	69.36	A	C	0
	A	D	69.36	A	E	15.20
	B	C	69.36	B	D	0
	B	E	71.60	D	C	69.36
	E	C	15.20	E	D	71.60
[Ir ₂ (H) ₄ (PPh ₃) ₄ (bted)](BF ₄) ₂ · 6CHCl ₃ (5 · 6CHCl ₃)	A	B	11.56	A	C	63.50
	A	D	63.50	A	E	11.56
	A	F	0	A	G	44.11
	B	C	54.68	B	D	54.68
	B	E	0	B	F	11.56
	B	G	37.88	C	D	0
	C	E	54.68	C	F	63.50
	C	G	71.41	D	E	54.68
	D	F	63.50	E	F	11.56
	G	D	71.41	G	E	37.88
G	F	44.11				
Metal free tptz ^a	A	D	15.7(1)	B	D	19.8(1)
	C	D	33.8(1)			
Metal-free tppz ^b	A	B	60.4	A	E	59.0
	D	E	46.4			
Metal-free tppz ^c	A	B	62.4	A	E	48.9
	D	E	51.7			

^a Ref. [23].

^b Ref. [24] (tetragonal form).

^c Ref. [24] (monoclinic form).



[Ir(tppz)Cl₃] [9e], [Cu(tppz)Cl₂] · CH₃CN [9f], [Cu(tppz)₂]ClO₄ [9f] and [Ni(tppz)₂](BF₄)₂ [9f] in the coordination mode (g). Although Re and Ru complexes

[Re(X)(CO)₃(tppz)] (X = Cl and Br) [8] and [Ru(phen)₂-(tppz)](PF₆)₂ [10] have recently been found as a mono-nuclear tppz complex in the coordination mode (f),

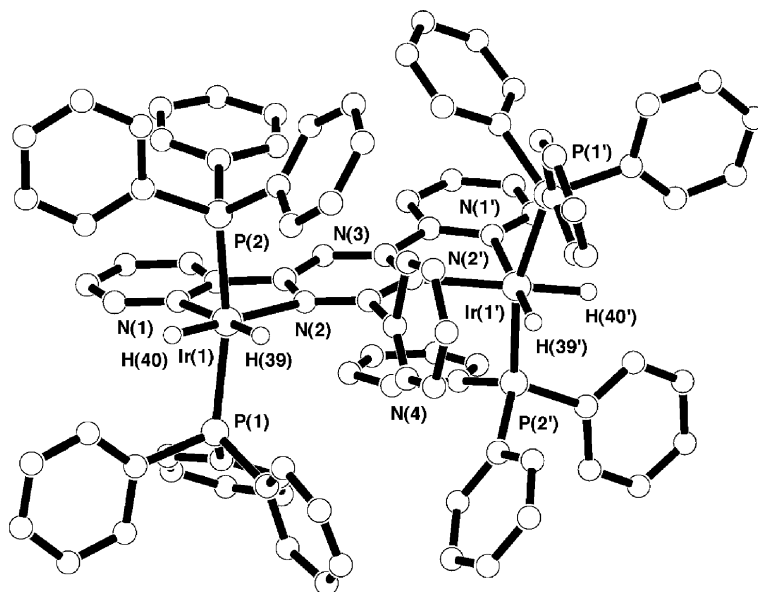


Fig. 3. The X-ray crystal structure of $[\text{Ir}_2(\text{H})_4(\text{PPh}_3)_4(\text{tptz})](\text{PF}_6)_2 \cdot 2\text{H}_2\text{O}$ (**2** · $2\text{H}_2\text{O}$).

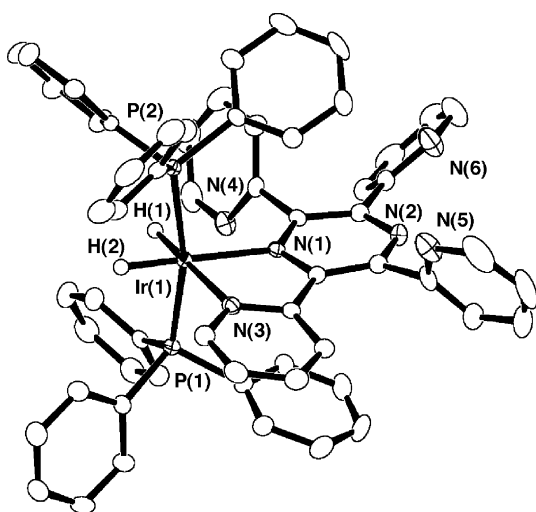


Fig. 4. The X-ray crystal structure of $[\text{Ir}(\text{H})_2(\text{PPh}_3)_2(\text{tppz})]\text{BF}_4$ (**3**).

complex **3** is the first tppz complex of Ir in the coordination mode (f).

The average Ir–P and Ir–N distances of 2.310 and 2.155 Å are close to those of other Ir–hydrido complexes with a nitrogen donor ligand [16b]. The Ir–H distances of 1.45(4) and 1.50(4) Å, and the H(1)···H(2) distance of 1.95 Å are similar to those of other Ir hydrido complexes with a nitrogen donor ligand [16b]. The N(1)–Ir(1)–N(3) angle is 76.5(1)°. The P(1)–Ir(1)–P(2) angle of 165.59(3)° is smaller than that (173.22(4)°) of mononuclear tppz complex **1**, indicative of the larger distortion from the octahedral geometry. In the metal-free tppz ligand, the dihedral angles between four pyridyl groups and the central pyrazine ring are {59.0° for rings (A) and (E), and 46.4° for rings (D) and (E)} for the tetragonal

form, and {48.9° for rings (A) and (E), and 51.7° for rings (D) and (E)} for the monoclinic form, respectively [24]. In the similar Re complex $[\text{ReCl}(\text{CO})_3(\text{tppz})] \cdot \text{MeOH}$ [8], it has also been reported that the uncoordinated pyridyl ring (D) is rotated at an angle of 59.0° with respect to the central pyrazine ring (E) and 56.7° with respect to the coordinated pyridyl ring (A). The coordinated pyridyl ring (A) is twisted 26.7° with respect to the central pyrazine ring (E). In contrast, in our complex **3**, the dihedral angle between the coordinated pyridyl ring (A) and the central pyrazine ring (E) is 12.06°, which is smaller than that of the $[\text{ReCl}(\text{CO})_3(\text{tppz})] \cdot \text{MeOH}$ complex [8]. The uncoordinated pyridyl ring (D) is rotated 67.58° and 73.23° against the central pyrazine ring (E) and the coordinated pyridine ring (A), respectively. It was obvious that the three uncoordinated groups were almost vertical against the central pyrazine ring (E) compared with the coordinated pyridyl ring (A). The selected bond distances, bond angles and dihedral angles are listed in Tables 2 and 3, respectively.

3.2.4. $[\text{Ir}_2(\text{H})_4(\text{PPh}_3)_4(\text{tppz})](\text{BF}_4)_2$ (**4**)

The 2:1 reaction of $[\text{Ir}(\text{H})_2(\text{PPh}_3)_2(\text{Me}_2\text{CO})_2]\text{BF}_4$ and tppz in Me_2CO provided dark-red crystals of **4**. The crystal structure of **4** is shown in Fig. 5 together with the atomic labeling scheme. The center of symmetry for complex **4** is at the middle of the central pyrazine ring. The tppz ligand acts as a bridging ligand, as does the tptz ligand in **2** · $2\text{H}_2\text{O}$. The two Ir atoms are coordinated by the four N atoms among the six potentially coordinative N atoms of tppz to form a dinuclear structure in the coordination mode (h). Each of the Ir atoms is coordinated by two *trans* PPh₃ ligands and two *cis* hydrido ligands in a distorted octahedral geometry.

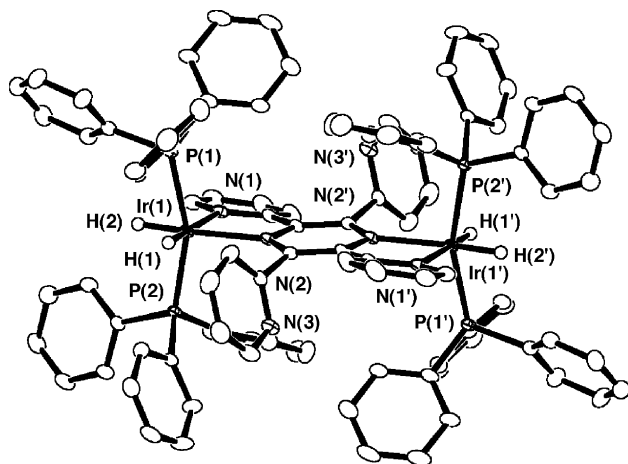


Fig. 5. The X-ray crystal structure of $[\text{Ir}_2(\text{H})_4(\text{PPh}_3)_4(\text{tppz})](\text{BF}_4)_2$ (**4**).

To the best of our knowledge, there are many dinuclear tppz complexes in the coordination mode (j): $[\text{Cu}_2(\text{H}_2\text{O})_2(\text{NO}_3)(\text{tppz})]^{2+}$ [9a], $[\text{Cu}_2\text{Cl}_4(\text{tppz})]$ [9a], $[\text{Cu}_2(\text{tppz})(\text{H}_2\text{O})_4](\text{ClO}_4)_4$ [9d], $[\text{Cu}_2(\text{tppz})\text{Cl}_2](\text{ClO}_4)_4$ [9d], $[\text{Pd}_2(\text{NO}_3)_2(\text{tppz})](\text{NO}_3)_2 \cdot 0.5\text{H}_2\text{O}$ [11a], $[\{\text{Cu}_2(\text{tppz})(\text{H}_2\text{O})_2$ [11b], *cis*- $[\text{Cl}(\text{dmb})\text{Ru}(\text{tppz})\text{Ru}(\text{dmb})\text{Cl}](\text{PF}_6)_2$ [11c], $[\text{Cu}_2(\text{tppz})\text{Cl}_4] \cdot 5\text{H}_2\text{O}$ [11d], $[\text{Ni}_2(\text{tppz})(\text{H}_2\text{O})_6](\text{NO}_3)_4 \cdot 2.5\text{H}_2\text{O}$ [11d], $[\text{Ni}_2(\text{tppz})(\text{H}_2\text{O})_6](\text{squarate})_2 \cdot 5\text{H}_2\text{O}$ [11d], $[\text{Zn}_5\text{Cl}_{10}(\text{tppz})(\text{H}_2\text{O})_2]$ [11e], $[\{(\mu\text{-Cl})_2(\text{MeCN})\text{Co}(\text{tppz})\text{Co}(\text{CoCl}_4)\}_n]$ [11f] and $[\{(\text{L}^4)\text{ClRu}\}_2(\text{tppz})(\text{ClO}_4)_2 \cdot 2\text{H}_2\text{O}$ [11g]. However, there are very few dinuclear complexes $[\{\text{ReBr}(\text{CO})_3\}_2(\mu\text{-tppz})]$ [8] in the coordination mode (h) and $[\{\text{Pt}(\text{PET}_3)\text{Cl}\}_2(\mu\text{-tppz})]$ $[\text{Pt}(\text{SnCl}_3)_4(\text{PET}_3)]$ [12] in the coordination mode (i), in addition to trinuclear complex $[\{\text{ReBr}(\text{CO})_3\}_3(\mu\text{-tppz})]$ in the coordination mode (k) [8]. Therefore, complex **3** is the first dinuclear Ir tppz complex to be identified in the coordination mode (h).

The average Ir–P and Ir–N distances of 2.315 and 2.178 Å are similar to those (2.310 and 2.155 Å) of **3**. The Ir–H distances of 1.40(3) and 1.37(3) Å, and the H(1)···H(2) distance of 1.83 Å are close to that of other

hydrido complexes [16a]. The N(1)–Ir(1)–N(2) angle is 75.32(6)°. The P(1)–Ir(1)–P(2) angle of 160.20(2)° is smaller than that of 173.22(4) (**1**) and 165.59(3)° (**3**). The dihedral angle of 15.20° between the coordinated pyridyl ring (A) and the central pyrazine ring (E) is distorted from the plane, whereas that between the uncoordinated pyridyl group (D) and the central pyrazine ring (E) is 71.60°. The selected bond distances, bond angles and dihedral angles are listed in Tables 2 and 3, respectively.

3.2.5. $[\text{Ir}_2(\text{H})_4(\text{PPh}_3)_4(\text{bted})](\text{BF}_4)_2 \cdot 6\text{CHCl}_3$ (**5** · 6CHCl₃)

According to the procedures in the experimental section, yellow brick crystals of **5** · 6CHCl₃ were collected. The crystal structure of **5** · 6CHCl₃ is shown in Fig. 6 together with the atomic labeling scheme. There is one $[\text{Ir}_2(\text{H})_4(\text{PPh}_3)_4(\text{bted})](\text{BF}_4)_2$ complex and six solvated CHCl₃ molecules in the unit cell. The center of symmetry for complex **5** · 6CHCl₃ is at the middle point of the central benzene ring in the bted ligand. Similar to complex **4**, the bted ligand acts as a bridging ligand to afford a dinuclear Ir hydrido complex by coordination of the four N atoms among the six possibly coordinative N atoms. Each of the Ir atoms is coordinated by two *trans* PPh₃ ligands and two *cis* hydrido ligands in a distorted octahedral geometry. Our survey in SciFinder showed no crystallographic study of metal bted complexes. There have been very few structural NMR studies of mononuclear bted complex $[\text{Pt}(\text{C}_6\text{F}_4\text{CF}_3)_2(\text{bted})]$ [13] in the coordination mode (l), and dinuclear bted complexes $[\{\text{Pt}(\text{C}_6\text{F}_4\text{CF}_3)_2\}_2(\text{bted})]$ [13], $[\{\text{ReBr}(\text{CO})_3\}_2(\text{bted})]$ [13], $[\{\text{Cp}^*\text{MCl}\}_2(\text{bted})](\text{BF}_4)_2$ (M = Rh and Ir) [14a] and $[\{\text{CpRu}(\text{PPh}_3)_2(\text{bted})]$ [14b] in the coordination mode (m). Therefore, this is the first crystallographic study of a metal complex with the bted ligand.

The average Ir–P and Ir–N distances of 2.300 and 2.158 Å are similar to those of complexes **1**, **2** · 2H₂O, **3** and **4**. The N(1)–Ir(1)–N(2) angle is 77.1(1)° and the P(1)–Ir(1)–

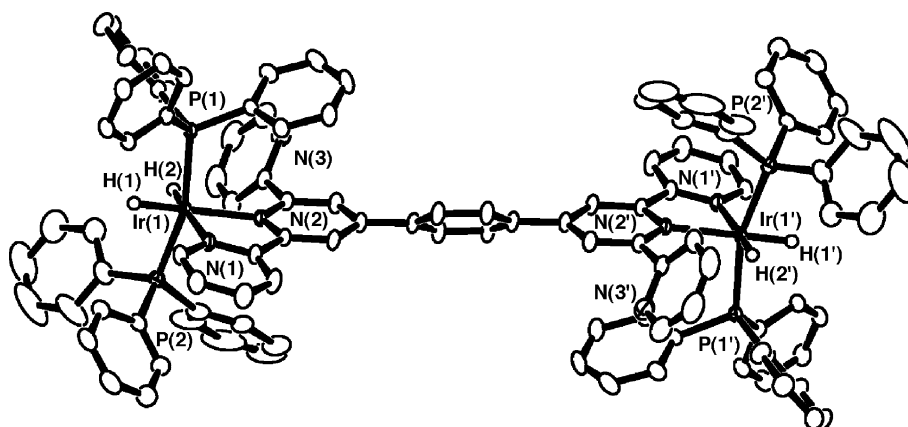


Fig. 6. The X-ray crystal structure of $[\text{Ir}_2(\text{H})_4(\text{PPh}_3)_4(\text{bted})](\text{BF}_4)_2 \cdot 6\text{CHCl}_3$ (**5** · 6CHCl₃).

P(2) angle of $161.84(3)^\circ$ is close to that ($160.20(3)^\circ$) of **4**. The Ir–H distances are 1.48(5) and 1.34(5) Å, and the H(1)···H(2) distance of 1.92 Å is slightly shorter than that (1.83 Å) of **4**. The dihedral angle of 11.56° between the coordinated pyridyl ring (A) and the pyridyl ring (B) is somewhat smaller than that (54.68°) between the uncoordinated pyridyl (C) ring and the pyridyl ring (B). The dihedral angle between the pyridyl ring (B) and the central benzene ring (G) is not coplanar at 37.88° . The selected bond distances, bond angles and dihedral angles are listed in Tables 2 and 3, respectively.

3.3. Dynamic structures in solution

3.3.1. Mono- and dinuclear Ir hydrido complexes with the tptz ligand, **1** and **2**·2H₂O

Complexes **1** and **2**·2H₂O showed quite complicated 1-D ¹H NMR signals in CD₂Cl₂ at 23 °C because three pyridyl groups of the tptz ligand and several phenyl groups of the PPh₃ ligands are simultaneously presented. We attempted to assign these signals by the use of ¹H–¹H COSY NMR techniques. The numberings for protons of each pyridine rings are denoted in the caption of Table 3. The ¹H–¹H COSY spectrum (Fig. 7) of

complex **1** suggests that there are three sets of four ¹H NMR signals that can be assigned to different pyridyl rings (A), (B) and (C), together with the overlapping ¹H NMR signals of PPh₃. The two coordinated hydrido atoms also showed two well-resolved ¹H NMR signals at -19.54 ($^1J_{\text{H-H}} = 8.2$ and $^2J_{\text{P-H}} = 16.1$ Hz) and -20.10 ($^1J_{\text{H-H}} = 8.2$ and $^2J_{\text{P-H}} = 14.6$ Hz) ppm. The correlations between each of the hydrido atoms and the P atom in the PPh₃ ligand could be confirmed by the ³¹P–¹H COSY NMR spectrum. The four proton atoms of the coordinated pyridyl ring (A) gave two doublet signals {8.62 (H¹) and 8.40 (H⁴) ppm}, one triplet signal {7.98 (H²) ppm} and the overlapping signal to PPh₃ {7.26 (H³) ppm}. These signals were shifted to the up-field region in comparison with those {8.92 (d, H^{4,8,12}), 8.81 (d, H^{1,5,9}), 7.99 (t, H^{2,6,10}) and 7.56 (t, H^{3,7,11}) ppm} of the metal-free tptz ligand. It is interesting that the H⁴ proton exhibited a larger shift of $\Delta\delta = 0.52$ ppm compared with those ($\Delta\delta = 0.01$ – 0.30 ppm) of the other ¹H NMR signals in the pyridyl ring (A). In contrast, the uncoordinated pyridyl ring (B), adjacent to the Ir core, exhibited two triplet signals {7.67 (H⁶) and 7.41 (H⁷) ppm}, a superimposed H⁸ signal (7.62 ppm) and a doublet signal {7.03 (H⁵) ppm}. It is remarkable that

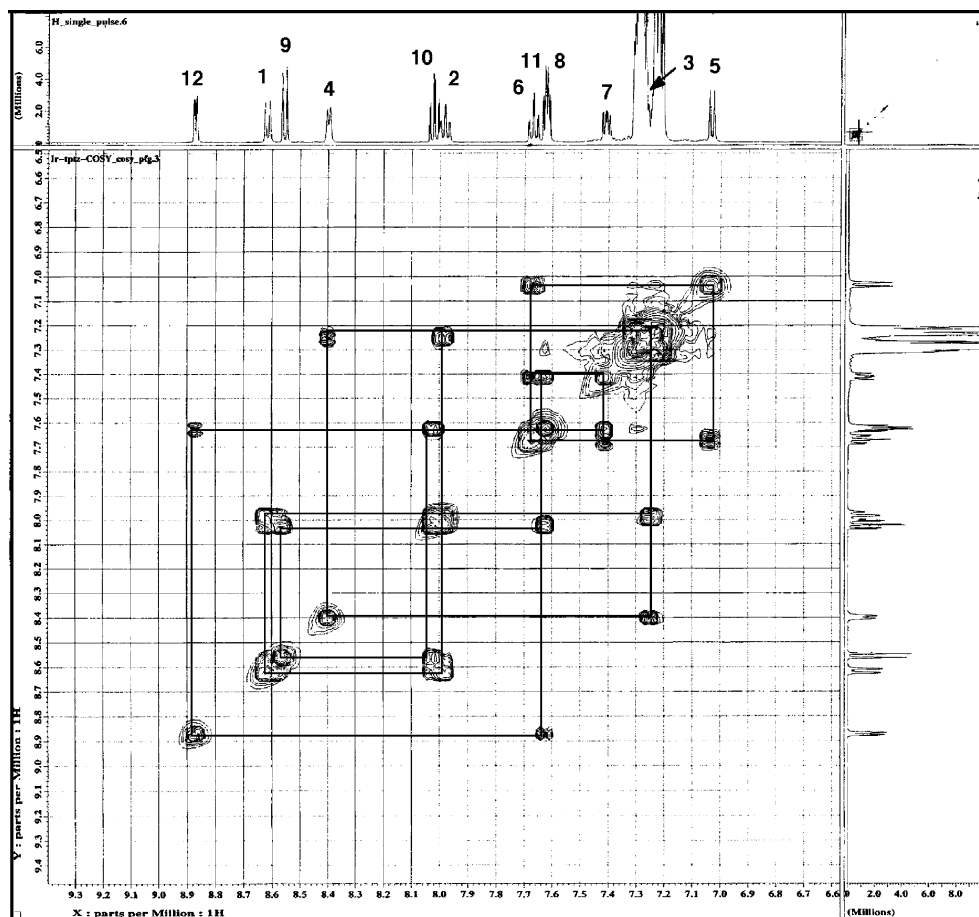


Fig. 7. ¹H–¹H COSY NMR spectrum in the aromatic region of [Ir(H)₂(PPh₃)₂(tptz)]PF₆ (**1**) in CD₂Cl₂ at 23 °C.

these signals were quite shifted to the up-field region ($\Delta\delta = 0.15\text{--}1.78$ ppm) compared with the metal-free tptz ligand. In particular, the H^5 signal represented an unusual up-field shift ($\Delta\delta = 1.78$ ppm). It is likely that shielding of the H^5 proton results from its interaction with the coordinated $[\text{Ir}(\text{H})_2(\text{PPh}_3)_2]$ fragment. Our crystallographic study showed that the uncoordinated pyridine ring (B) of complex **1** is surrounded by phenyl groups of the neighboring PPh_3 . These findings seem to indicate that the uncoordinated pyridyl ring (B) is highly shielded by the neighboring PPh_3 ligands to give a larger up-field shift, as it appears that the neighboring CO ligands could not significantly contribute to the shielding or deshieldings by the ring current effect in similar mononuclear Re complex $[\text{ReX}(\text{CO})_3(\text{tptz})]$ ($X = \text{Cl}$ and Br) [3e] with the coordination mode (b). When predicting the ^1H NMR shifts of complex **1** on the basis of the crystallographic study, the pyridine ring (A) was assumed to give the largest up-field shift among the pyridyl rings (A), (B) and (C) due to the contribution of the largest ring current effects of the PPh_3 group. However, our NMR study indicated that the pyridyl ring (B) had a larger up-field shift ($\Delta\delta = 0.15\text{--}1.78$ ppm) than that ($\Delta\delta = 0.01\text{--}0.52$ ppm) in the pyridyl ring (A). It is thought that the up-field shift based on the ring current effect is compensated for the down-field shift based on the coordination shift of the Ir atom to the pyridyl ring (A), resulting in a decrease of the up-field shifts. Finally, the ^1H NMR signals of the remaining uncoordinated pyridine ring (C) at $\{8.87$ (d, H^{12}), 8.56 (d, H^9), 8.02

(t, H^{10}) and 7.62 (t, H^{11}) ppm} were essentially unshifted with respect to those of the metal-free tptz ligand. This behavior is similar to that observed in the mononuclear Re complex $[\text{ReX}(\text{CO})_3(\text{tptz})]$ [3e]. It is interesting that the shift ($\Delta\delta = 0.25$ ppm) of the H^9 proton is larger than those ($\Delta\delta = 0.03\text{--}0.05$ ppm) of other ^1H NMR signals.

In complex **2**· $2\text{H}_2\text{O}$, the $^1\text{H}\text{--}^1\text{H}$ COSY spectrum exhibited two sets (intensity ratio 2:1) of four ^1H NMR signals assignable to 12 pyridyl protons in the tptz ligand (Fig. 8), which is the number expected for two magnetically equivalent coordinated pyridyl rings (A) and (B) and one nonequivalent pyridyl ring (C). Contrary to complex **1**, two hydrido atoms in **2**· $2\text{H}_2\text{O}$ showed multiple ^1H NMR signals at -20.65 ppm, indicative of an overlapping of two hydrido signals. The coordinated pyridyl rings (A) and (B) showed two doublet signals $\{8.61$ ($H^{1,5}$) and 7.56 ($H^{4,8}$) ppm}, one triplet signal $\{8.07$ ($H^{2,6}$) ppm} and the overlapping signal to PPh_3 $\{7.15$ ($H^{3,7}$) ppm}. The shift ($\Delta\delta = 1.36$ ppm) at the $H^{4,8}$ position in pyridyl rings (A) and (B) is larger than that ($\Delta\delta = 0.49$ ppm) of the corresponding complex **1**. Furthermore, the uncoordinated pyridyl ring (C) showed two triplet signals $\{7.50$ (H^{11}) and 7.34 (H^{10}) ppm}, the superimposed H^{12} signal (7.47 ppm) and the doublet signal $\{6.29$ (H^9) ppm}. It is worth nothing that these signals were unusually shifted to the up-field region ($\Delta\delta = 0.06\text{--}2.52$ ppm). In particular, the larger up-field shift of $\Delta\delta = 2.52$ ppm at the H^9 position than that ($\Delta\delta = 0.25$ ppm) in complex **1** is surprising. In similar dinuclear Ru and Os complexes with the tptz ligand

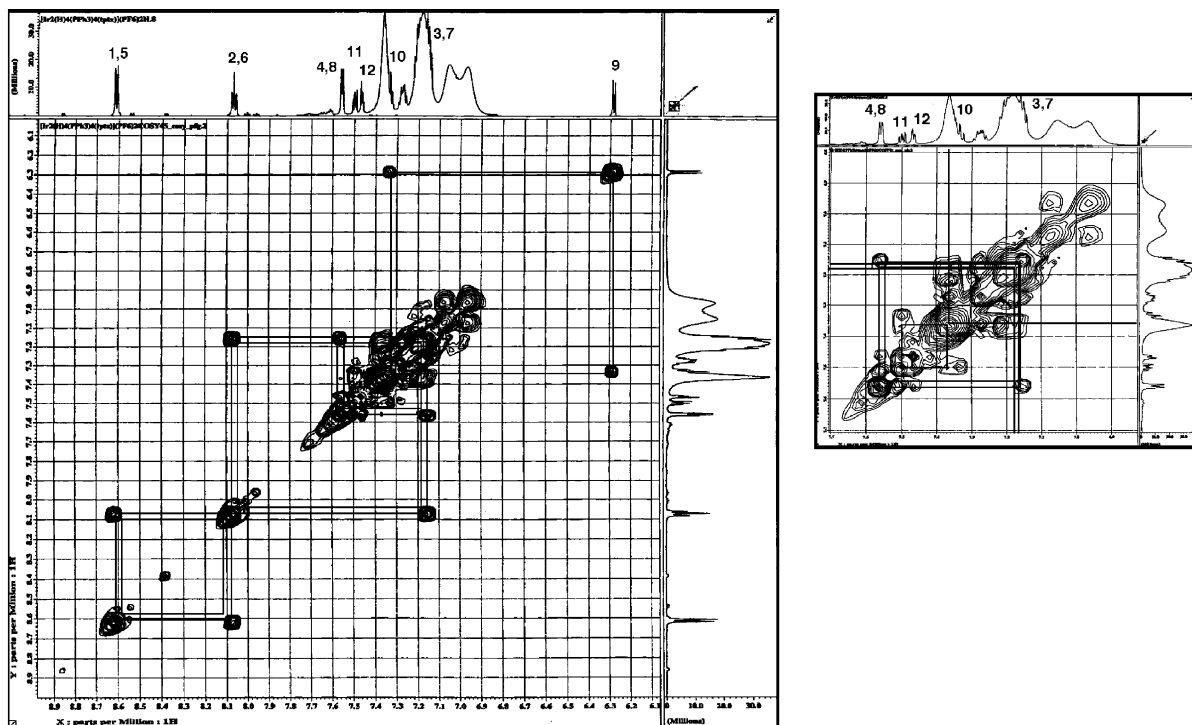


Fig. 8. $^1\text{H}\text{--}^1\text{H}$ COSY NMR spectrum in the aromatic region of $[\text{Ir}_2(\text{H})_4(\text{PPh}_3)_4(\text{tptz})](\text{PF}_6)_2 \cdot 2\text{H}_2\text{O}$ (**2**· $2\text{H}_2\text{O}$) in CD_2Cl_2 at 23°C .

rac-[M(bpy)₂]₂(tptz-H)(PF₆)₃ (M = Ru and Os) [3d], it has been reported that the signals of the uncoordinated pyridine ring (C) in the coordinated tptz ligand exhibit the up-field shifts of { $\Delta\delta = 2.80$ (H⁹), 1.84 (H¹⁰), 1.19 (H¹¹) and 2.17 (H¹²) ppm}. These behaviors have been explained as being ring current effects produced by the neighboring 2,2'-bipyridine ligands. Our crystallographic study of complex **2** showed that the uncoordinated pyridyl ring (C) is close to the Ph groups in the neighboring PPh₃ and other pyridyl rings in the tptz ligand. As with complex **1**, it is thought that unusual chemical shifts are likely induced by the ring current effects of the neighboring ligands. The detailed ¹H NMR chemical shifts of complexes **1** and **2**·2H₂O are listed in Table 4.

3.3.2. Mono- and dinuclear Ir hydrido complexes with the tppz ligand, **3** and **4**

Complex **3** showed 16 well-resolved ¹H NMR signals of the tppz ligand in CD₂Cl₂ at 23 °C together with ¹H NMR signals (7.26 ppm) of the PPh₃ ligands. The ¹H–¹H COSY NMR techniques described four sets of ¹H NMR signals that can be assigned to different pyridyl rings (A), (B), (C) and (D) in the tppz ligand. To assign each of the pyridyl rings (A)–(D), ¹H–¹H ROESY NMR techniques were also employed. The results show that ¹H NMR signals of PPh₃ are obviously correlated to the H⁴ atom in the pyridyl ring (A) and the H^{13,16} atoms in the pyridyl ring (D). Furthermore, the H¹ atom in the pyridyl ring (A) is related to the H⁵ atom in the pyridyl ring (B). The H⁸ and H⁶ atoms in the pyridyl ring (B) are related to the H^{11,12} and H¹⁰ atoms in the pyridyl ring (C), respectively. These findings indicate that the pyridyl rings (A) and (D) are located close to the Ph groups of the coordinated PPh₃ ligands. The pyridyl ring (A) is neighboring the pyridyl rings {(B) and (D)} and the pyridyl ring (B) is close to the pyridyl ring (C). Uncoordinated pyridyl rings (B), (C) and (d) can be fluxional in solution and their orientation is different from those in the solid state. On the basis of these correlations and the assignments of complexes **1** and **2**·2H₂O, the assignments of four pyridyl rings (A)–(D) were finally defined as the scheme in the caption of Table 3. The two coordinated hydrido atoms showed two well-resolved ¹H NMR signals at –19.48 (¹J_{H–H} = 7.9 and ²J_{P–H} = 17.4 Hz) and –20.67 (¹J_{H–H} = 7.6 and ²J_{P–H} = 14.6 Hz) ppm. Detailed ¹H NMR chemical shifts of complex **3** are listed in Table 4. Similar to complexes **1** and **2**, ¹H NMR signals of the uncoordinated pyridyl ring (D), adjacent to the Ir core, indicate a larger up-field shift ($\Delta\delta = 0.13$ –2.58 ppm) compared with those of the metal-free tppz ligand. In particular, it is surprising that the H¹³ signal represents an unusual up-field shift ($\Delta\delta = 2.58$ ppm), which is larger than those ($\Delta\delta = 1.78$ and 2.52 ppm) of complexes **1** and **2**. The ¹H NMR signals of the coordinated pyridyl ring (A) showed an

up-field shift ($\Delta\delta = 0.26$ –1.30 ppm), although these signals should apparently be canceled by the down-field shift based on the coordination shift. The H¹ proton exhibits a shift of $\Delta\delta = 1.30$ ppm, which is larger than that ($\Delta\delta = 0.52$ ppm) of the H⁴ proton in complex **1**. The uncoordinated pyridyl rings (B) and (C) also show smaller shifts of $\Delta\delta = 0.05$ –0.27 and 0.17–0.49 ppm, respectively. Although it is expected that ¹H NMR signals of the uncoordinated pyridine rings (B) and (C) should be nearly unshifted, these signals were partially shifted by each current ring effect and the coordination shift to the Ir atom.

In contrast to mononuclear tppz complex **3**, dinuclear tppz complex **4** redissolved in CD₂Cl₂ showed two kinds of ¹H NMR signals at 23 °C. The major species exhibited the broadened ¹H NMR signals at {8.39, 7.61, 6.47 and 6.32 ppm} for pyridyl groups in the tppz ligand and at {–19.12 and –20.95 ppm} for the two hydrido atoms together with those of the PPh₃ ligands at {7.32 and 7.16 ppm}, whereas the minor species presented the well-resolved ¹H NMR signals of complex **3**. These behaviors indicate that dinuclear tppz complex **4** is partially dissociated in CD₂Cl₂ to afford a small amount of complex **3**. The variable-temperature ¹H NMR spectra were measured to determine the broadened species at low temperature (Fig. 9). At –90 °C, the broadened species could be separately observed as well as the six well-resolved ¹H NMR signals at {8.53, 7.66, 7.63, 6.40, 6.29 and 6.04 ppm} and the two ¹H NMR signals for the two hydrido atoms at {–18.85 and –21.70 ppm}, together with those of complex **3**. These signals could be assigned by the ¹H–¹H COSY NMR techniques as follows: the coordinated pyridyl rings (A) and (C) showed the two doublet signals {8.53 (H^{4,12}) and 6.04 (H^{1,9}) ppm} and two triplet signals {7.66 (H^{3,11}) and 7.63 (H^{2,10}) ppm}, whereas the uncoordinated pyridyl rings (B) and (D) gave one doublet signal {6.40 (H^{8,16}) ppm} and one triplet signal {6.29 (H^{6,14}) ppm} together with two overlapping signals {7.13 (H^{7,15}) and 7.03 (H^{5,13}) ppm} to PPh₃. At present, the specific dissociation process of complex **4** is not clear. However, suggesting by the variable-temperature ¹H NMR spectra, it is considered that two Ir atoms in complex **4** are instantaneously replaced between the two coordination sites formed by the central pyrazine ring and pyridyl rings {(A) and (C)} and other pyridyl rings {(B) and (D)}, since the major species **4** showed the broad ¹H NMR signals at room temperature and relatively sharp ¹H NMR signals with lower temperatures. A small amount of complex **3** should be produced on this fluxional behavior. The resultant complex **3** is stably kept in CD₂Cl₂ without the reformation to complex **4**, since the minor species **3** showed the well-resolved ¹H NMR signals even at room temperature. These findings could be supported by the presence of fluxional behaviors in mono- and dinuclear complexes with tptz [6b,25a,25b] and betd ligands [13,14a]. It is

Table 4

Spectroscopic data of mono- and dinuclear Ir hydrido complexes with polydentate nitrogen ligands, 1–5 · 6CHCl₃

Compounds	¹ H NMR ^a (Δδ, ppm)	UV–Vis ^c (λ _{max} , nm)	IR(Ir–H) ^c (cm ⁻¹)
[Ir(H) ₂ (PPh ₃) ₂ (tptz)]PF ₆ (1) ^a	{8.62(d, H ¹), 8.40 (d, H ⁴), 7.98 (dt, H ²) and 7.26 (t, H ³)} for ring (A); {7.67 (dt, H ⁶), 7.62 (dd, H ⁸), 7.41 (dt, H ⁷) and 7.03 (d, H ⁵)} for ring (B); {8.87 (dddd, H ¹²), 8.56 (td, H ⁹), 8.02 (dt, H ¹⁰) and 7.62 (dt, H ¹¹)} for ring (C); 7.27 (m, PPh ₃); –19.54 (dt, Ir–H) and –20.10 (dt, Ir–H)	400, 480	2250, 2205
[Ir ₂ (H) ₄ (PPh ₃) ₄ (tptz)](PF ₆) ₂ · 2H ₂ O (2 · 2H ₂ O) ^a	{8.61(d, H ^{1,5}), 8.07 (dt, H ^{2,6}), 7.56 (d, H ^{4,8}) and 7.15 (dt, H ^{3,7})} for rings (A) and (B); {7.50 (dt, H ¹¹), 7.47 (dddd, H ¹²), 7.34 (dt, H ¹⁰) and 6.29 (dd, H ⁹)} for ring (C); 7.22 (m, PPh ₃); –20.65 (m, Ir–H)	430, 510	2248
[Ir(H) ₂ (PPh ₃) ₂ (tppz)]BF ₄ (3) ^a	{8.10(d, H ⁴), 7.30 (t, H ²), 6.76 (dt, H ³) and 6.73 (d, H ¹)} for ring (A); {8.56 (dddd, H ⁸), 8.09 (dt, H ⁶), 7.98 (td, H ⁵) and 7.55 (dt, H ⁷)} for ring (B); {8.16 (dddd, H ¹²), 7.62 (dt, H ¹⁰), 7.54 (dd, H ⁹) and 7.11 (dt, H ¹¹)} for ring (C); {7.51 (dddd, H ¹⁶), 7.17 (dt, H ¹⁴), 7.15 (dt, H ¹⁵) and 5.45 (td, H ¹³)} for ring (D); 7.26 (m, PPh ₃); –19.48 (dt, Ir–H) and –20.67 (dt, Ir–H)	360, 465	2291, 2192
[Ir ₂ (H) ₄ (PPh ₃) ₄ (tppz)](BF ₄) ₂ (4) ^{a,d}	{8.39(br), 7.61 (br), 6.47 (br) and 6.32 (br)} for tppz; 7.32 (br, PPh ₃), 7.16 (br, PPh ₃); –19.12 (t, Ir–H) and –20.95 (t, Ir–H) at 23 °C. {8.53 (d, H ^{4,12}), 7.66 (dt, H ^{3,11}), 7.63 (t, H ^{2,10}) and 6.04 (d, H ^{1,9})} for rings (A) and (C); {7.13 (H ^{7,15}) and 7.03 (H ^{5,13}), 6.40 (d, H ^{8,16}) and 6.29 (t, H ^{6,14})} for rings (B) and (D); –18.85 (dt, Ir–H) and –21.70 (dt, Ir–H) at –90 °C.	375, 535	2284, 2233
[Ir ₂ (H) ₄ (PPh ₃) ₄ (btcd)](BF ₄) ₂ · 6CHCl ₃ (5 · 6CHCl ₃) ^b	{8.55(d, H ^{1,13}), 8.49 (d, H ^{4,16}), 7.98 (t, H ^{3,15}) and 7.15 (dt, H ^{2,14})} for rings (A) and (F); {8.54(d, H ^{9,21}) and 7.68 (d, H ^{10,22})} for rings (B) and (E); {7.64 (d, H ^{8,20}), 7.59 (dt, H ^{6,18}), 7.41 (dt, H ^{7,19}) and 6.29 (d, H ^{5,17})} for rings (C) and (D); 8.19 (s, H ^{11,12,23,24}) for ring (G); 7.37 (m, PPh ₃); –19.30 (dt, Ir–H) and –20.22 (dt, Ir–H)	310, 400	2282
Metal-free tptz ^a	8.92 (dddd, H ^{4,8,12}), 8.81 (dddd, H ^{1,5,9}), 7.99 (dt, H ^{2,6,10}) and 7.56 (dt, H ^{3,7,11})		
Metal-free tppz ^a	8.36 (dddd, H ^{4,8,12,16}), 8.03 (dddd, H ^{1,5,9,13}), 7.84 (dt, H ^{2,6,10,14}) and 7.28 (dt, H ^{3,7,11,15}) at 23 °C. 8.31 (d, H ^{4,8,12,16}), 7.99 (d, H ^{1,5,9,13}), 7.85 (t, H ^{2,6,10,14}) and 7.28 (t, H ^{3,7,11,15}) at –90 °C.		
Metal-free btcd ^c	8.81 (s, H ^{9,10,21,22}), 8.77 (dddd, H ^{4,8,16,20}), 8.71 (dddd, H ^{1,5,13,17}), 8.07 (s, H ^{11,12,23,24}), 7.91 (dt, H ^{2,6,14,18}) and 7.37 (dt, H ^{3,7,15,19})		

^a In CD₂Cl₂ at 23 °C.^b In (CD₃)₂CO at 23 °C.^c In CDCl₃ at 23 °C.^d ¹H NMR signals of a small amount of complex **3** were simultaneously observed.^e In the solid state with KBr disk.

interesting that the coordinated pyridyl rings (A) and (C) exhibited a larger shift (Δδ = 0.22–1.95 ppm) at –90 °C compared with ¹H NMR signals {8.31, 7.99, 7.85 and 7.28 ppm} of the metal-free tppz ligand. In particular, it is surprising that the H^{1,9} signals represented the unusual up-field shift (Δδ = 1.95 ppm). In contrast, the uncoordinated pyridyl rings (B) and (D), adjacent to the Ir core, gave the up-field shifted ¹H NMR signals of Δδ = 1.91 (H^{8,16}) and 1.56 (H^{6,14}) ppm. Similar to the ¹H NMR spectra of complexes 1–3, these results suggest that unusual shifts should be induced by the ring current effect on the basis of the crystallographic features of complex **4**.

The detailed ¹H NMR chemical shifts of complexes **3** and **4** are summarized in Table 4.

3.3.3. Dinuclear Ir hydrido complexes with the betd ligand, 5 · CHCl₃

Complex **5** · 6CHCl₃ exhibited 11 well-resolved ¹H NMR signals in the betd ligand in (CD₃)₂CO at 23 °C, that could be assigned to pyridyl rings (A), (B), (C) and (G) in the betd ligand by ¹H–¹H COSY NMR techniques. The well-resolved ¹H NMR spectrum indicated that a dinuclear structure is maintained at room temperature without the dissociation and the

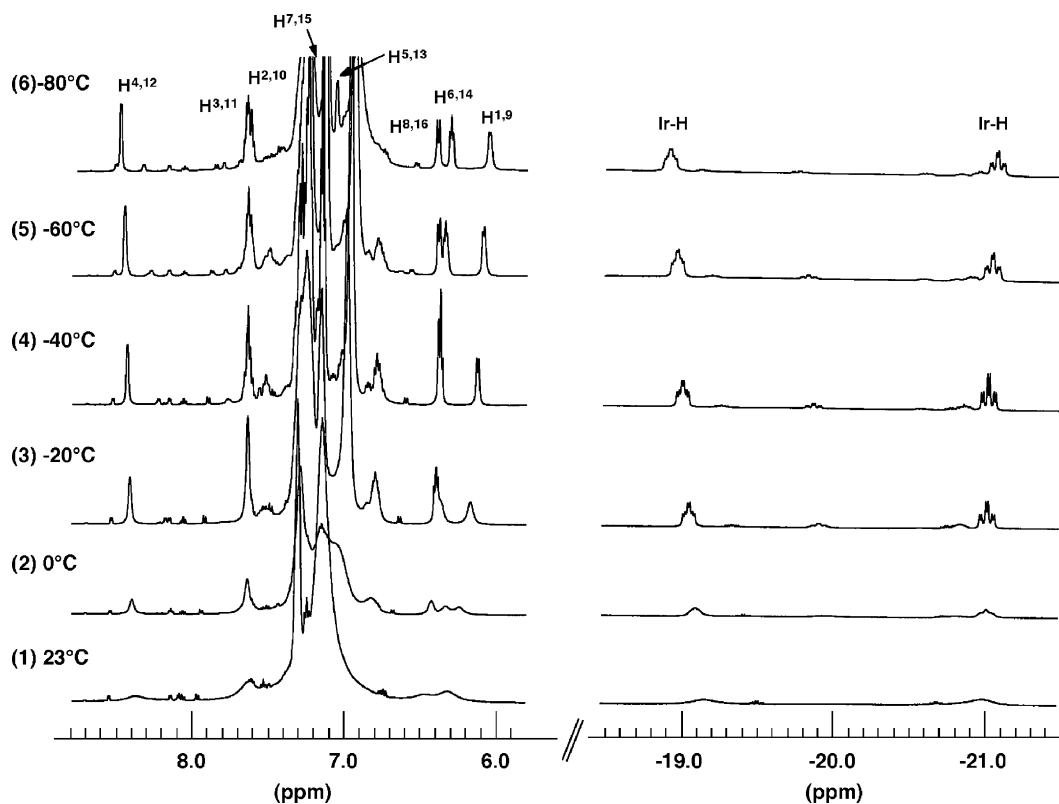


Fig. 9. The variable-temperature ^1H NMR spectra of $[\text{Ir}_2(\text{H})_4(\text{PPh}_3)_4(\text{tppz})](\text{BF}_4)_2$ (**4**) in CD_2Cl_2 .

equilibrium. In the NMR study of dinuclear btd complexes $[\{\text{Pt}(\text{C}_6\text{F}_4\text{CF}_3)_2\}_2(\text{btd})]$ [13], $[\{\text{Re}-\text{Br}(\text{CO})_3\}_2(\text{btd})]$ [13], and $[(\text{Cp}^*\text{MCl})_2(\text{btd})](\text{BF}_4)_2$ ($\text{M} = \text{Rh}$ and Ir) [14a], fluxional behaviors have been reported among several species at ambient and high temperatures. The dynamic behaviors of Ir complex **5**· 6CHCl_3 are different than those of other btd complexes [13, 14a], suggesting that Ir complex **5**· 6CHCl_3 is not labile in $(\text{CD}_3)_2\text{CO}$. The two hydrido signals were observed at -19.30 ($^1J_{\text{H-H}} = 7.6$ and $^2J_{\text{P-H}} = 17.0$ Hz) and -20.22 ($^1J_{\text{H-H}} = 7.8$ and $^2J_{\text{P-H}} = 15.4$ Hz) ppm. The coordinated pyridyl rings {(A) and (F)} showed ^1H NMR signals at $\{8.55$ (d, $\text{H}^{1,13}$), 8.49 (d, $\text{H}^{4,16}$), 7.98 (t, $\text{H}^{2,14}$) and 7.15 (t, $\text{H}^{3,15}$) ppm}, whereas the uncoordinated pyridyl rings {(C) and (D)} exhibited well-resolved ^1H NMR signals at $\{7.64$ (d, $\text{H}^{8,20}$), 7.59 (t, $\text{H}^{6,18}$), 7.41 (t, $\text{H}^{7,19}$) and 6.29 (d, $\text{H}^{5,17}$) ppm}. The ^1H NMR resonances of rings {(B) and (E)} and (G) were also exhibited at $\{8.54$ (d, $\text{H}^{9,21}$), 7.68 (d, $\text{H}^{10,22}$); and 8.19 (s, $\text{H}^{11,12,23,24}$) ppm, respectively, together with that (7.37 (m, PPh_3) ppm) of PPh_3 . ^1H NMR signals of the uncoordinated pyridyl rings (C) and (D), adjacent to the Ir core, showed the largest up-field shift ($\Delta\delta = 0.5$ – 2.42 ppm) among the other signals, with the $\text{H}^{5,17}$ signals having the largest up-field shift ($\Delta\delta = 2.42$ ppm). The detailed ^1H NMR chemical shifts of complex **5**· 6CHCl_3 were summarized in Table 4.

In summary, a series of Ir hydrido complexes with polydentate nitrogen ligands gave well-resolved ^1H

NMR signals except for complex **4** at room temperature. The complex **4** showed interesting fluxional behaviors at low temperature. All of the dynamic structures in solution demonstrated that the ring current effect should primarily be reflected in the chemical shifts of each pyridyl ring in polydentate nitrogen ligands. In particular, it was found that the uncoordinated pyridyl ring, adjacent to the Ir core, has the larger up-field shift due to the ring current effect.

4. Supplementary materials

Crystallographic data for the X-ray crystal structural analysis have been deposited with the Cambridge Crystallographic Data Center, CCDC, Nos. 209702 – 209706 for complexes **1**, **2**· $2\text{H}_2\text{O}$, **3**, **4** and **5**· 6CHCl_3 , respectively. Copies of this information may be obtained free of charge from The Director, CCDC, 12 Union Road, Cambridge, CB2 1EZ, UK (fax: +44-1233-336033; e-mail: deposit@ccdc.cam.ac.uk or www.hutter-phenyl://www.ccdc.cam.ac.uk).

Acknowledgements

We thank Mr. T. Morita, Mr. T. Kanzaki and Mr. D. Tomomatsu for their assistance. This work was partially supported by a Grant-in-Aid for Scientific Research

from the Ministry of Education, Science, Sports, Culture and Technology of Japan.

References

- [1] (a) M.A. Fox, M. Chanon (Eds.), *Photoinduced Electron Transfer*, Elsevier, New York, 1988;
 (b) T.J. Meyer, *Acc. Chem. Res.* 22 (1989) 163;
 (c) T.J. Meyer, in: N. Kitamura (Ed.), *Photochemical Process in Organized Molecular Systems*, Elsevier, Amsterdam, 1991;
 (d) V. Balzani, F. Scandola (Eds.), *Supramolecular Photochemistry*, Horwood, Chichester, UK, 1991.
- [2] (a) C. Musikas, W.W. Schulz, in: J. Rydberg, C. Musikas, G.R. Choppin (Eds.), *Principles and Practices of Solvent Extraction*, 413, Marcel Dekker, New York, 1992 (Chapter 11);
 (b) C. Musikas, X. Vitart, J.Y. Pasquiou, P. Hoel, in: C.J. King, J.D. Navratil (Eds.), *Chemical Separations*, vol. 2, Litarvan Literature, Denver, 1986, p. 358.
- [3] (a) P. Paul, B. Tyagi, M.M. Bhadbhade, E. Suresh, *J. Chem. Soc., Dalton Trans.* (1997) 2273;
 (b) P. Paul, B. Tyagi, A.K. Bilakhiya, M.M. Bhadbhade, E. Suresh, *J. Chem. Soc., Dalton Trans.* (1999) 2009;
 (c) P. Paul, B. Tyagi, A.K. Bilakhiya, M.M. Bhadbhade, E. Suresh, G. Ramachandraiah, *Inorg. Chem.* 37 (1998) 5733;
 (d) P. Paul, B. Tyagi, A.K. Bilakhiya, P. Dastidar, E. Suresh, *Inorg. Chem.* 39 (2000) 14;
 (e) X. Chen, F.J. Femia, J.W. Babich, J.A. Zubieta, *Inorg. Chem.* 40 (2001) 2769.
- [4] (a) W.A. Embry, G.H. Ayres, *Anal. Chem.* 40 (1968) 1499;
 (b) M.J. Janmohamed, G.H. Ayres, *Anal. Chem.* 44 (1972) 2263.
- [5] (a) N.C. Thomas, B.L. Foley, A.L. Rheingold, *Inorg. Chem.* 27 (1988) 3426;
 (b) S. Chirayil, V. Hegde, Y. Jahng, R.P. Thummel, *Inorg. Chem.* 30 (1991) 2821;
 (c) N. Gupta, N. Grover, G.A. Neyhart, P. Singh, H.H. Thorp, *Inorg. Chem.* 32 (1993) 310;
 (d) R.M. Berger, J.R. Holcombe, *Inorg. Chim. Acta* 232 (1995) 217.
- [6] (a) M.G.B. Drew, M.J. Hudson, P.B. Iveson, C. Madic, *Acta Crystallogr., Sect. C* 56 (2000) 434;
 (b) R. Wietzke, M. Mazzanti, J.-M. Latour, J. Pécaut, *Inorg. Chem.* 38 (1999) 3581;
 (c) J.M. Harrowfield, H. Miyamae, B.W. Skelton, A.A. Soudi, A.H. White, *Aust. J. Chem.* 49 (1996) 1157;
 (d) P. Byers, G.Y.S. Chan, M.G.B. Drew, M.J. Hudson, *Polyhedron* 15 (1996) 2845.
- [7] H.A. Goodwin, F. Lyons, *J. Am. Chem. Soc.* 81 (1959) 6415.
- [8] X. Chen, F.J. Femia, J.W. Babich, J.A. Zubieta, *Inorg. Chim. Acta* 315 (2001) 66.
- [9] (a) Z. Baloghova, J. Kozisek, M. Koman, D. Valigura, *Monogr. Ser. Int. Conf. Coord. Chem.* 3 (1997) 99;
 (b) M.F. Ahmet, B. Coutinho, J.R. Dilworth, J.R. Miller, S.J. Parrott, Y. Zheng, *Polyhedron* 15 (1996) 2041;
 (c) P. Lainé, A. Gourdon, J.-P. Launay, *Inorg. Chem.* 34 (1995) 5156;
 (d) M. Graf, B. Greaves, H. Stoeckli-Evans, *Inorg. Chim. Acta* 204 (1993) 239;
 (e) L.M. Vogler, B. Scott, K.J. Brewer, *Inorg. Chem.* 32 (1993) 898;
 (f) H. Bock, H. Schödel, T. Vaupel, *Z. Naturforsch.* 52b (1997) 515.
- [10] C. Metcalfe, S. Spey, H. Adams, J.A. Thomas, *J. Chem. Soc., Dalton Trans.* (2002) 4732.
- [11] (a) Y. Yamada, Y. Miyashita, K. Fujisawa, K. Okamoto, *Bull. Chem. Soc. Jpn.* 73 (2000) 1843;
 (b) D. Hargrman, P. Hargrman, J. Zubieta, *Inorg. Chim. Acta* 300 (2000) 212;
 (c) C.M. Hartshorn, N. Daire, V. Tondreau, B. Loeb, T.J. Meyer, P.S. White, *Inorg. Chem.* 38 (1999) 3200;
 (d) M. Graf, H. Stoeckli-Evans, A. Escuer, R. Vicente, *Inorg. Chim. Acta* 257 (1997) 89;
 (e) M. Graf, H. Stoeckli-Evans, *Acta. Crystallogr., Sect. C* 50 (1994) 1461;
 (f) E.C. Constable, A.J. Edwards, D. Phillips, P.R. Raithby, *Supramol. Chem.* 5 (1995) 93;
 (g) N. Chanda, R.H. Laye, S. Chakraborty, R.L. Paul, J.C. Jeffery, M.D. Ward, G.K. Lahiri, *J. Chem. Soc., Dalton Trans.* (2002) 3496;
 (h) J.K. Bera, C.S. Campos-Fernández, C. Rodolphe, K.R. Dunbar, *J. Chem. Soc., Chem. Commun.* (2002) 2536.
- [12] W.M. Teles, N.L. Speziali, C.A.L. Filgueiras, *Polyhedron* 19 (2000) 739.
- [13] A. Gelling, M.D. Olsen, K.G. Orrell, A.G. Osborne, V. Sik, *J. Chem. Soc., Dalton Trans.* (1998) 3479.
- [14] (a) H. Aneetha, P.S. Zacharias, S. Srinivas, G.H. Lee, Y. Wang, *Polyhedron* 18 (1998) 299;
 (b) K.M. Rao, C.R.K. Rao, P.S. Zacharias, *Polyhedron* 16 (1997) 2369.
- [15] P.A. Chaloner, M.A. Esteruelas, F. Joó, L.A. Oro, *Homogeneous Hydrogenation*, Kluwer, Dordrecht, 1994.
- [16] (a) X.-Y. Yu, M. Maekawa, M. Kondo, S. Kitagawa, G.-X. Jin, *Chem. Lett.* (2001) 168;
 (b) X.-Y. Yu, M. Maekawa, T. Morita, H.-C. Chang, S. Kitagawa, G.-X. Jin, *Bull. Chem. Soc. Jpn.* 75 (2002) 267;
 (c) X.-Y. Yu, M. Maekawa, T. Morita, H.-C. Chang, S. Kitagawa, G.-X. Jin, *Polyhedron* 21 (2002) 1613.
- [17] (a) O.W. Howarth, C.H. McAtee, P. Moore, G.E. Morris, *J. Chem. Soc., Dalton Trans.* (1981) 1481;
 (b) R.H. Crabtree, P.C. Demou, D. Eden, J.M. Mihelcic, C.A. Parnell, J.M. Quirk, G.E. Morris, *J. Am. Chem. Soc.* 104 (1982) 6994.
- [18] (a) SAPI-91: Fan Hai-Fu, *Structure Analysis Programs with intelligent Control*, Rigaku Corporation, Tokyo, Japan, 1991;
 (b) SIR-92: A. Altomara, M.C. Burla, M. Camelli, M. Cascarano, C. Giacovazzo, A. Guagliardi, G. Polidori, *J. Appl. Cryst.* 27 (1994) 435.
- [19] DIRDIF-94: P.T. Beurskens, G. Admiraal, G. Beurskens, W.P. Bosman, R. de Gelder, R. Israel, J.M.M. Smits, *The DIRDIF-94 program system*, Technical Report of the Crystallography Laboratory, University of Nijmegen, 1994.
- [20] D.T. Cromer, J.T. Waber, in: *International Tables for X-Ray Crystallography*, vol. IV, Kynoch Press, Birmingham, 1974.
- [21] TEXSAN, *Crystal Structure Analysis Package*, Molecular Structure Corporation 1985 and 1999.
- [22] (a) P.H. Jessop, R.H. Morris, *Coord. Chem. Rev.* 121 (1992) 151;
 (b) F.A. Cotton, G. Wilkinson, C.A. Murillo, M. Bochmann, *Advanced Inorganic Chemistry*, sixth ed., Wiley, New York, 1999, pp. 1097–1096.
- [23] M.G.B. Drew, M.J. Hudson, P.B. Iveson, M.L. Russell, C. Madic, *Acta Crystallogr., Sect. C* 54 (1998) 985.
- [24] B. Greaves, H. Stoeckli-Evans, *Acta Crystallogr., Sect. C* 48 (1992) 2269.
- [25] (a) A. Gelling, M.D. Olsen, K.G. Orrell, A.G. Osborne, V. Sik, *J. Chem. Soc., Chem. Commun.* (1997) 587;
 (b) A. Gelling, M.D. Olsen, K.G. Orrell, A.G. Osborne, V. Sik, *Inorg. Chim. Acta* 264 (1997) 257.